TL552
.M41
.F614 no. 66-5

# APPLICATION OF THE CALCULUS OF VARIATIONS IN DETERMINING OPTIMUM FLIGHT PROFILES FOR COMMERCIAL SHORT HAUL AIRCRAFT

R. Gallant

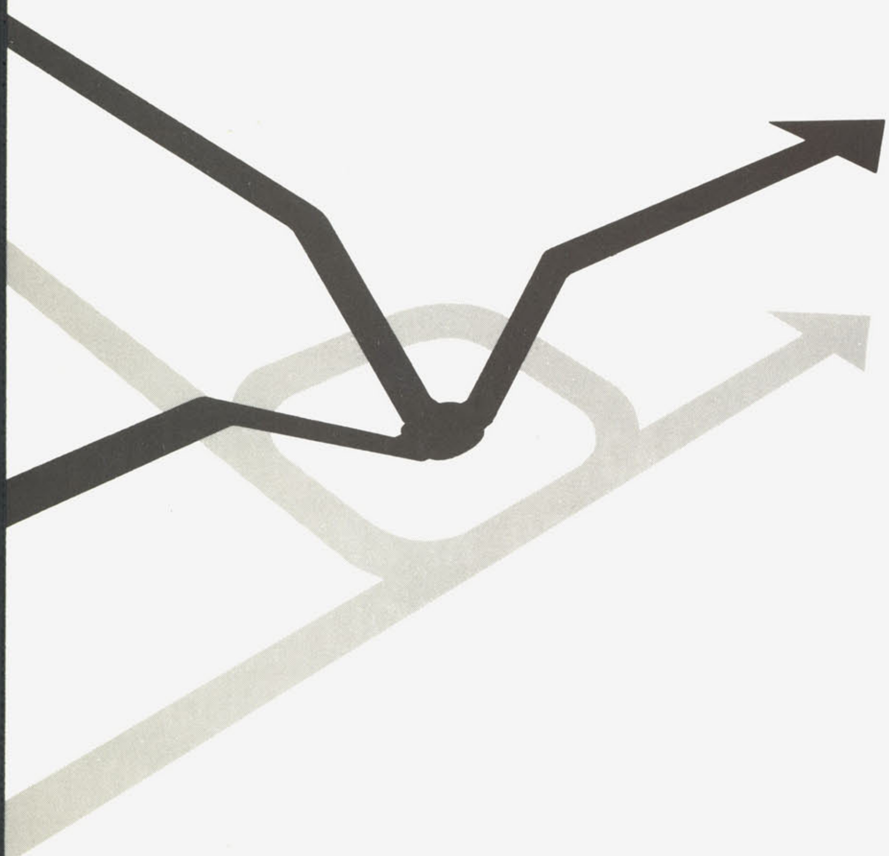

FT-66-5

**DEPARTMENT OF AERONAUTICS & ASTRONAUTICS**

**FLIGHT TRANSPORTATION LABORATORY**

Prepared for the U.S. Department of Commerce under Contract C-85-65

NOVEMBER 1966

ARCHIVES

MASSACHUSETTS INSTITUTE OF TECHNOLOGY

FLIGHT TRANSPORTATION LABORATORY

Technical Report FT-66-5

December, 1966

Robert A. Gallant

# APPLICATION OF THE CALCULUS OF VARIATIONS IN DETERMINING OPTIMUM FLIGHT PROFILES FOR COMMERCIAL SHORT HAUL AIRCRAFT

This work was performed under Contract C-136-66 for the Office of High Speed Ground Transport, U. S. Department of Commerce.

## ABSTRACT

The method of steepest descent of the calculus of variations is used to determine the optimal flight profile of a hypothetical tilt wing aircraft travelling a distance of 50 miles. Direct operating cost, (as derived from the ATA formulation) is minimized using aircraft lift coefficient and power as control variables each with upper and lower limits. Only the portion of the flight from the end of transition to the beginning of retransition was considered, with both initial and final values of velocity, flight path angle, and altitude specified.

The results show that full power is used to accelerate and to climb at a speed about twice the value for maximum rate of climb. At 12000 feet, power is reduced to flight idle and a high speed, power off glide is made to destination. A rapid deceleration is made at low altitude to achieve the specified conditions for retransition. While the optimal profiles for velocity, altitude, and power are greatly different from the nominal profiles chosen to design the aircraft (Ref. 5), the optimal trip cost of $30.54 is only slightly less than the nominal trip cost of $31.60.

TABLE OF CONTENTS

# CHAPTER I

## INTRODUCTION

Airlines have long been faced with the question of how to operate their aircraft most economically. An important aspect of this question is that of what altitude and velocity profile should be flown so as to minimize direct operating cost (DOC). This report presents a mathematical optimization technique for determining optimal altitude and velocity profiles which will result in minimum direct operating cost for a flight of any given range.

Many aircraft optimal profile problems have been solved where either fuel or time were minimized. For the problem treated here, where direct operating cost is to be minimized, the DOC is approximated by a linear combination of fuel burned and time of flight since the controllable cost of a flight are linearly related to these factors. The coefficients of this linear equation are empirical and are based on airline experience with various types of aircraft.

Historically, long range aircraft have been designed and flown with emphasis placed on the cruise portion of the flight. Formerly, aircraft were designed and flown at an altitude and velocity which resulted in maximum lift to drag ratio and the objective was to minimize fuel consumption. In recent years, however, airlines have come to realize the overall cost advantage of high speed flight, where there exists the potential of increased utilization and lower DOC per flight. For example, high speed operation results in the saving of crew and maintenance costs per flight since these costs are, for the most part, based on flight time, not distance. Modern long range aircraft are, of course, still designed with emphasis placed on the cruise portion of the flight, since this constitutes a major portion of a long range trip. For these aircraft, optimum cruise is usually at high speed and high altitude, and is specifically described by the aircraft manufacturer for every user. The time and fuel penalties of climbing and accelerating to these cruise conditions are generally small in comparison to the gains of optimal cruise, and a variety of climb and descent profiles are used by different airlines for the same type of aircraft.

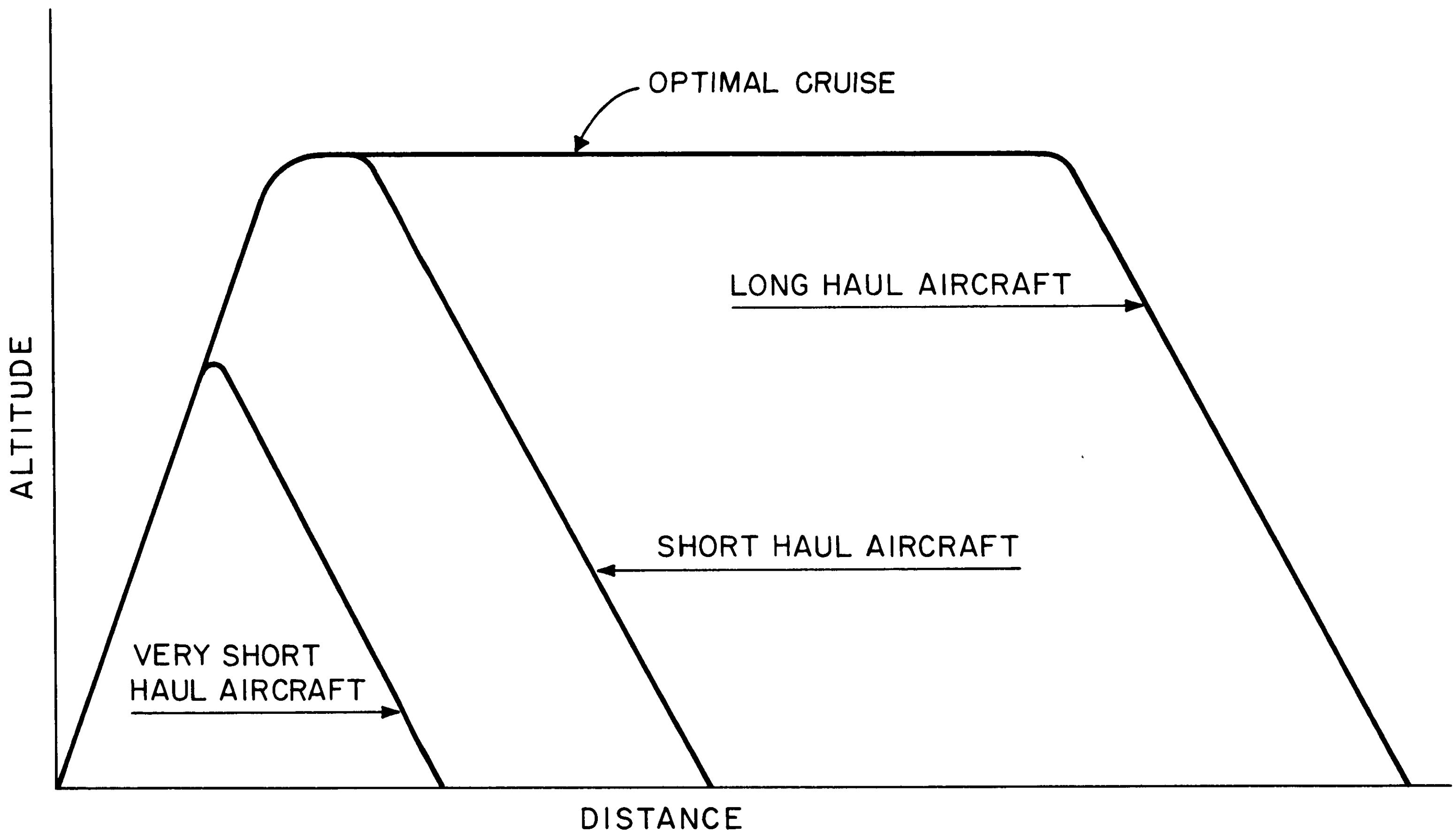


Figure 1. Typical Altitude Profiles for Various Flight Distances of Commercial Aircraft (not to scale).

With the potential advent of short haul and very short haul aircraft, this operating philosophy is no longer valid. For example, it can be seen in Figure 1 that an attempt to fly a commercial short haul aircraft at a high altitude cruise condition is impractical if not impossible. If a high cruise altitude can be attained, the benefits of efficient cruise generally may not be worthwhile, since the short time of cruise flight may not offset the cost of climbing to this altitude. For very short haul aircraft, high cruise altitudes will never be attained because of the short trip length. Since the costly climb phase is now a major portion of the total flight profile, the question of what total integrated altitude and velocity profile should be flown to minimize direct operating cost is now confronted.

In the studies of the possible future application of VSTOL aircraft for the Northeast Corridor described in Ref. 5, the question of which profile should be used in the design procedures was answered in a typical engineering manner. Various selections of cruise were made for various ranges, and the aircraft were climbed at a speed for maximum rate of climb. It was recognized however, that these selections of speed and altitude were probably non-optimal and that they were a sensitive input to both the design of the vehicles and the cost of their operation particularly at shorter ranges. Arguments could be proposed for various profiles, and the profiles could be tested, but it was clear that the questions could never be resolved satisfactorily unless an attempt was made to use rigorous mathematical methods for determining least cost profiles. Even if the resulting profiles were impractical because of passenger comfort, or air traffic control reasons, the knowledge of how to use the excess power of the VTOL vehicles in speed and height profiles was needed to direct the selection of simple and feasible profiles for the engineering design. This report describes the effort to apply present methods from the calculus of variations to solve such a problem for a Tilt wing aircraft travelling a distance of 50 miles from the end of transition to wing borne flight to the beginning of re-transition. The method can be applied to flight profile optimization for any type of short haul aircraft.

# CHAPTER II

## TECHNICAL APPROACH

The technique set forth in this report to the solution of this problem is the method of steepest descent in the calculus of variations. Basically, the technique involves commencing with a guess of a nominal flight control history which will result in a reasonable flight profile. Small changes in the control history are then made so as to change the flight profile from the nominal in a direction that will reduce the performance index (the DOC in this case). This procedure is repeated until no further reduction in performance index is possible. The control history and flight profile are then considered optimal. Since the aircraft system equations are very nonlinear, the aid of a computer is mandatory in the solution of this problem. The theoretical aspects of the technique are presented in Appendix A.

A hypothetical short haul vertical takeoff and landing (VTOL) tilt wing commercial aircraft is used in the demonstration of the flight profile optimization technique. A description of this vehicle is presented in Section 2.1. An empirical formulation based on the Air Transport Association of America direct operating cost formula is used to relate DOC to aircraft design and operating characteristics. This formulation is presented in Section 2.2. Section 2.3 presents the aircraft system equations and the formulation of these equations for computer solution of the optimal profile. Appendix B describes the computer programming procedure. Successful computerization of a theoretical approach to the solution of a problem is not always straight forward. This is particularly true with regards to numerical stability and accuracy. With this in mind, Appendix B describes the program and highlights some of the important computational problems. Some of the computational procedures used can probably be successfully applied to the solution of similar steepest descent problems.

## 2.1 Aircraft Description

A hypothetical commercial short haul vertical takeoff and landing tilt wing aircraft with four turbo-shaft engines powering propellers is used in the demonstration of the flight profile optimization technique. The significant design parameters of the aircraft are presented in Figure 2. This aircraft design was derived from research conducted for the U.S. Department of Commerce to determine the feasibility of commercial short haul air transportation in the Northeast Corridor of the United States[5,6].

The aircraft has a design range of 200 statute miles. However, as with other types of commercial aircraft, it will at times operate at less than this range. In fact, flights of 50 miles or less are envisioned. For these short ranges, it is reasonable to assume that the aircraft will not operate at its design cruise velocity or altitude anywhere along its flight path. However, it is not obvious what profiles this aircraft should fly for optimum operation. A 50 mile range

# DESCRIPTION OF HYPOTHETICAL COMMERCIAL SHORT HAUL VTOL TILT WING AIRCRAFT

| | |
|---|---|
| Design Range | 200 St. miles |
| Design Altitude | 20,000 ft. |
| Design Velocity | 400 m.p.h. |
| Gross Weight, $W_{gr}$ | 57,244 lb. |
| Number of Passengers | 80 |
| Crew | Pilot and Copilot |
| Payload | 16,600 lb. |
| Engine Normal Rated Power, NRP | 18,800 H.P. @ S.L. |
| Engines | 4 turboshaft |
| $SFC_o$, specific fuel consumption @ S.L. and NRP | .55 lb. of fuel per hr./HP |
| Propeller-Transmission efficiency, $\eta$ | .72 |
| Engine weight, $W_E$ | 3539 lb. |
| Fuel weight | 4080 lb. |
| Oil weight | 140 lb. |
| Wing area, WAR | 686.5 sq. ft. |
| Wing efficiency factor, e | .85 |
| Aspect Ratio, AR | 9.5 |
| Profile Drag Coefficient, $C_{D_o}$ | .024917 |

Figure 2

case is evaluated to illustrate a typical solution to this problem. The aircraft is assumed to fly in a two dimensional vertical plane, since direct flight between two locations is considered.

The 50 mile flight optimization is calculated for the segment of flight where the aircraft is in a conventional flight mode, that is, from the end of transition (takeoff phase) to the beginning of retransition (landing phase). Ideally, the optimization technique should be performed from lift-off to touch-down. However, excluding the transition and retransition phases of flight (where the wing is at an angle other than zero degrees) does not detract from the demonstration of the technique or the realism of the problem since these phases constitute a very small portion of the total flight time, distance, and fuel burned for this type of aircraft. The main advantage of this simplification is the elimination of wing angle as a control variable and avoidance of nonlinear equations required to describe the flow field over the wing at low forward speeds and high wing angles.

The aircraft control variables used in the optimization program were lift coefficient, $C_L$, and power level, designated as Power. The lift coefficient was considered to be the most practical variable to use in controlling the aircraft in the direction normal to its flight path. In actual operation, control in this direction is accomplished by variation of wing angle of attack, $\alpha$, and the use of flaps. The choice of $C_L$, therefore, combined two control variables into one and, consequently, eliminated complex interrelated control of $\alpha$ and flap position. The profile drag coefficient, $C_{D_O}$, has been taken to be constant for all lift coefficients even though this assumption is slightly wrong in the case where flaps would need to be used. However, the resultant error in drag at this flight condition is negligible. The lift coefficient was limited to a maximum value of 3.0, which is a practical upper limit for an aircraft using auxiliary high lift devices. The magnitude of the control variable Power was based on "equivalent sea level horsepower" and limited to a maximum value of normal rated power (NRP = 18,800 horsepower) and a minimum value of 10% NRP. The later limit was based on the requirement that a minimum positive power level must be maintained to keep the engines operating at idle and this appeared to be a practical lower limit for current turboshaft engines. The former limit was chosen for the sake of simplicity even though it is possible to operate turboshaft engines above NRP for short periods of time.

The engine fuel flow rate, Q, was based on typical turboshaft engine experience. It is a function of Power level and altitude as presented below.

$$Q = P_{alt} \frac{SFC}{3600}$$

where $P_{alt}$ is the altitude corrected engine power and is empirically formulated as

$$P_{alt} = \text{Power}(1 - \frac{.55h}{30,000})$$

SFC is the specific fuel consumption at power level Power and is also empirically formulated as

$$SFC = SFC_o \left[\frac{NRP}{Power}\right]^{.36}$$

Substituting, we obtain

$$Q = \frac{SFC_o}{3600} (\text{Power})^{.64} (\text{NRP})^{.36} (1 - \frac{.55h}{30,000})$$

The propeller thrust is based on simple momentum theory where the propeller is treated as an actuator disc with a propeller-transmission efficiency $\eta$. It is formulated as

$$T = \frac{550 \, P_{alt} \eta}{V}$$

Substituting for $P_{alt}$ results in

$$T = \frac{550 (\text{Power}) \eta \, (1 - \frac{.55h}{30,000})}{V}$$

In addition to the reasons presented earlier, the determination of the optimal profile for this type of aircraft is also particularly interesting since it has a large power to weight ratio required for vertical take-off and landing and is, therefore, overpowered for the conventional mode of flight. It is not obvious whether the aircraft should use the total excess power available in this mode. If the excess power is used to attain high velocity, the aircraft may suffer a penalty of high fuel costs. On the other hand, operating at lower levels, and therefore lower velocity, could result in high time costs. Determining the proper balance between these two extremes over the total integrated flight profile is accomplished by the optimization program.

The initial and final aircraft flight conditions specified for the optimized portion of the flight profile were selected to be

Velocity

$$V(t_o) = V(t_f) = 160 \text{ fps}$$

Flight Path Angle:

$$\gamma(t_o) = \gamma(t_f) = 0 \text{ radians}$$

Altitude:

$$h(t_o) = h(t_f) = 3500 \text{ feet}$$

The altitude was selected on the basis of having adequate clearance above the ground for safe aircraft operation during wing conversion (moving the wing with respect to the fuselage in transition). The flight path angle was selected on the basis that wing conversion would probably be performed in level flight. The velocity was selected so that the lift coefficient would be near its maximum allowed value at the beginning and end of the conventional portion of the flight.

The propeller efficiency was taken to be constant at .8. No reduction of efficiency due to compressibility effects was made since the maximum velocity was not that large. The transmission efficiency was taken to be .9 which resulted in a combined propeller-transmission efficiency, $\eta$, of .72.

## 2.2 Formulation of Performance Index

The performance index, $\Phi$, is based on an estimate of the direct operating cost of the tilt wing VTOL aircraft. The DOC of an aircraft owned by a particular airline is determined by their operational experience. However, for the aircraft considered here, the direct operating cost was based on average industry experience. This experience has been empirically formulated by the Air Transport Association of America (ATA)[4].

Broadly speaking, the DOC can be divided into two major components, fuel cost and time cost. The time cost can be subdivided into cost of

1. Oil
2. Crew
3. Direct Maintenance
4. Applied Maintenance Burden
5. Depreciation
6. Insurance

The importance and control of the cost of each of these elements is a function of the time base in which they are being evaluated. For example, applied maintenance burden is the cost for maintenance facilities and is fixed in the short run. If the time base was several years, or the life of a fleet of aircraft, this cost would be variable, and, therefore, controllable. The time period being considered in this problem is the time of one 50 mile flight (less than 15 minutes). Therefore, the cost of applied maintenance burden is not part of the performance index, that is, the performance index is only a function of the controllable elements of the short term DOC. Depreciation is considered fixed for the same reason. Since the cost of insurance is based on miles flown, it is also a fixed cost. Therefore, only items 1 through 3 are considered controllable since they are in whole or in part a function of the time of flight. An evaluation of these three costs plus fuel costs is presented below. The equations presented are a summary of the pertinent ATA empirical cost relationships.

Fuel Cost

The cost of fuel, b, for the turboshaft engines was taken to be .01743 dollars per pound. The fuel used was assumed to be JP-4 with a density of 6.5 pounds per gallons and a cost of 0.1133 dollars per gallon (domestic rate, including tax). Therefore, the total cost of fuel for the optimized segment of the flight profile was

$$\text{Fuel Cost} = \int_{t_o}^{t_f} bQ\, dt$$

where Q is the fuel flow rate in pounds per second and t is in seconds.

Oil Cost

The cost of oil is a function of the time of flight since the rate of oil consumption is taken to be 2/3 pounds per hour per engine. The oil density is assumed to be 8.1 pounds per gallon with a cost of 6.20 dollars per gallon. Therefore, the cost of oil for this four engine aircraft is

$$\text{Oil Cost} = \int_{t_o}^{t_f} \frac{2.045}{3600}\, dt$$

Crew Cost

A crew of two is assumed; pilot and copilot. The cost of both crew members consists of an annual base rate plus adjustments for such factors as the number of hours flown, the number of miles flown, and the aircraft gross weight. The airline operator must also take into account allowances for such indirect costs as vacations, training, and over-nighting expenses. Some of these crew costs are not functions of flight time and, therefore, are not inputs to the performance index. Since it would serve no purpose to elaborate on the details of the crew costs and the structure of its formulation, a summary of the controllable components of this cost is presented below. The aircraft gross weight factor has not been combined with the other terms to allow for the possibility of changes in the aircraft design.

$$\text{Crew Cost} = \int_{t_o}^{t_f} \frac{28.06 + 4.637\times10^{-5}\, W_{gr}}{3600}\, dt$$

$W_{gr}$ is the aircraft gross weight.

Direct Maintenance

Direct maintenance cost is divided into maintenance of engines and maintenance of aircraft. Aircraft maintenance includes the airframe plus all related equipment such as radios and navigation equipment. These direct maintenance costs are further subdivided into labor costs and material costs. The formulation of these costs is presented below.

Engine Labor Cost

The empirical equation for engine labor cost is

$$\text{Engine Labor Cost} = \int_{t_o}^{t_f} \frac{3.09\,(NE)\,(K_{LE})}{3600}\, dt$$

where

$NE$ = number of engines = 4

The coefficient 3.09 is the labor cost in dollars per man-hour and $K_{LE}$ is the labor required in man-hours per flight hour per engine. The later is formulated as

$$K_{LE} = \frac{545.16 + .05852\ (ESHP)}{TBO} + .1$$

where

ESHP = equivalent shaft horsepower = 1.053 (NRP)

TBO = time between overhaul = 4000 hours

<u>Aircraft Labor Cost</u>

The empirical equation for aircraft labor cost is

$$\text{Aircraft Labor Cost} = \int_{t_o}^{t_f} \frac{3.09\ K_{LA}}{3600}\, dt$$

Again, the coefficient of 3.09 is the labor cost in dollars per man-hour. The constant $K_{LA}$ is the aircraft labor required in man-hours per flight hour and is formulated as

$$K_{LA} = 3.0 + 6.7 \times 10^{-5}\ W_A$$

where $W_A$ is the basic weight of the aircraft less engine weight. It is determined by subtracting the weight of payload, fuel, engines, and oil from the gross weight.

Engine Material Cost

The engine material cost is determined by

$$\text{Engine Material Cost} = \int_{t_o}^{t_f} \frac{K_{ME}(NE)}{3600}\, dt$$

where $K_{ME}$ is the cost of materials in dollars per flight hour per engine and is empirically formulated as

$$K_{ME} = \frac{5.59\times10^{-5}(CE)(SPF) - 0.484}{K_{TBO}}$$

where

$CE$ = cost of one engine

$= 300\ (W_E)/(NE)$

$W_E$ = Weight of all engines

$SPF$ = Spare Parts Factor = 1.5

$K_{TBO} = 2.1 \times 10^{-4}(TBO) + 0.769$

The formulation of $K_{TBO}$ is used to relate the cost of materials with time between overhauls.

Aircraft Materials Cost

$$\text{Aircraft Material Cost} = \int_{t_o}^{t_f} \frac{K_{MA}}{3600}\, dt$$

$K_{MA}$ is the cost of aircraft materials in dollars per flight hour and is empirically formulated as

$$K_{MA} = 2.58 + 8.14 \times 10^{-6} C_A$$

where

$$C_A = \text{cost of aircraft less engines}$$
$$= 68.2\ W_A$$

Cost Summary

The controllable portion of the direct operating cost (performance index) can be summarized as follows:

$$\Phi = \int_{t_o}^{t_f} \dot{z}\ dt$$

where

$$\dot{z} = a + bQ$$

and

$$a = (43.67 + 4.637 \times 10^{-5}\ W_{gr} + 7.62 \times 10^{-4}\ W_A$$
$$+ .01563\ W_E + 1.90 \times 10^{-4}\ NRP)/3600$$

Substituting the design parameters of the short haul tilt wing aircraft results in

$$a = .03620\ \ \$/\text{second}$$

Also

$$b = .01743\ \ \$/\text{lb}$$

## 2.3 System Equations

Formulation of the system equations and associated equations required for the solution of the optimal flight profile is performed in this section. The system equations describe the dynamics of the aircraft and its operating characteristics. The associated equations are required for the steepest descent optimization process as described in Appendix A. These equations were programmed for digital computation as presented in Appendix B.

The aircraft has been modeled as a point mass since the aircraft pitch dynamics are at a much higher frequency than the flight path dynamics. If the aircraft pitch mode had been included as part of the system dynamics, the resultant optimal solution would have been essentially the same. As shown in Figure 3, the thrust is assumed to always act along the flight path. This assumption serves to simplify the equation formulation and introduces very little error. The relationship of the other system variables is also shown in this figure.

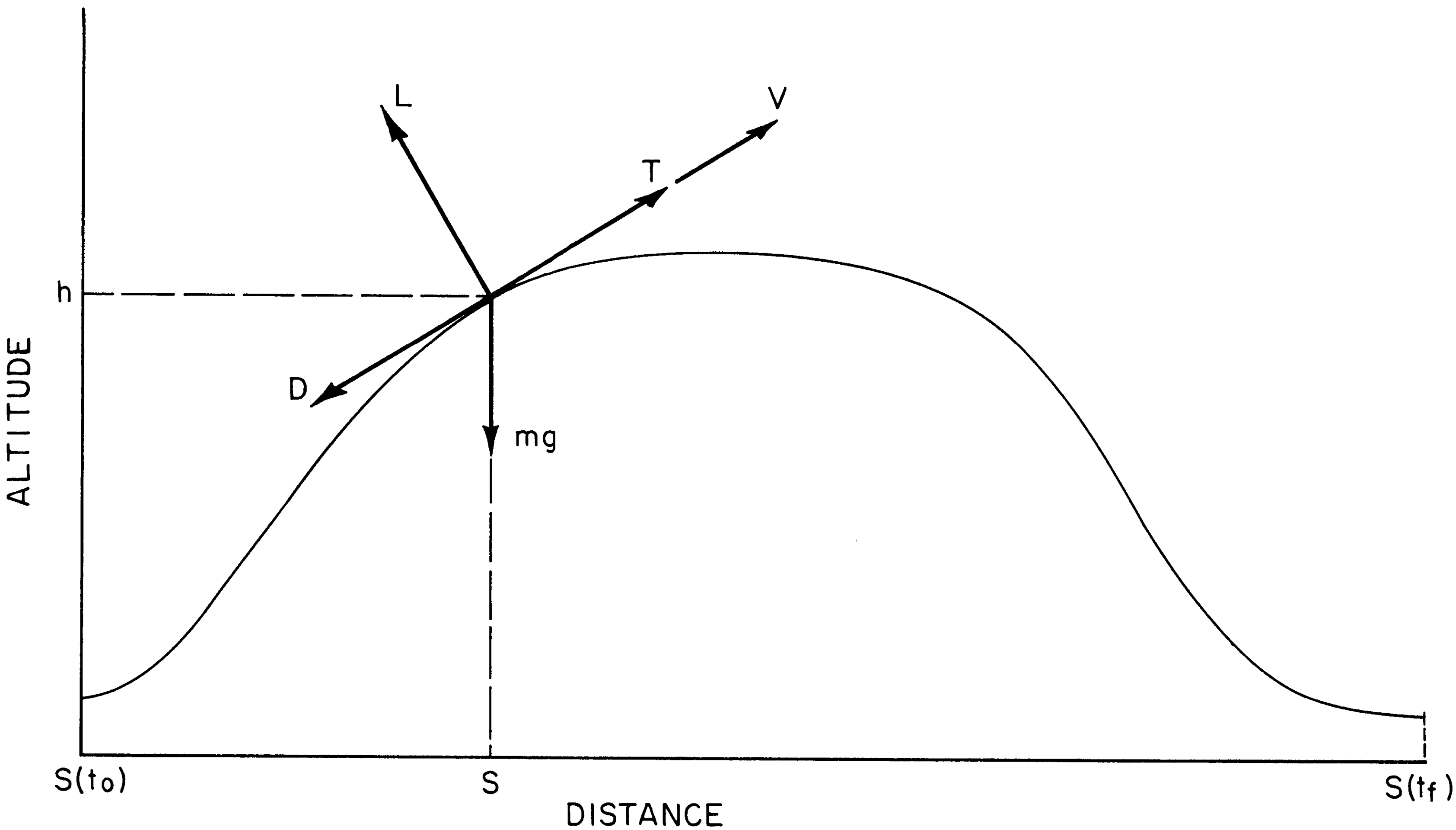


Figure 3. Relationship of System Variables

Several other assumptions that were made are as follows. The gross weight was taken to remain constant even though fuel was being burned throughout the flight. This is a reasonable assumption since the fuel burned in a 50 mile flight only amounts to about one per cent of the gross weight. Also, incompressible flow is assumed for both airframe and propellor operation since the maximum velocity attained was not unreasonably high. The flight path was considered to be in the vertical plane only, and zero wind velocity was assumed. Also, there were no state variable inequality constraints, as might be required if there had been air traffic control limitations.

In the initial phases of research for this report, time, t, was taken to be the independent variable and the equations of motion of the aircraft were

$$\dot{V} = \frac{T-D}{m} - g \sin \gamma$$

$$\dot{\gamma} = \frac{L}{mV} - \frac{g}{V} \cos \gamma$$

$$\dot{h} = V \sin \gamma$$

$$\dot{s} = V \cos \gamma$$

Since the performance index was, in part, a function of time, and the stopping condition a function of distance, the time vector had a variable length. Therefore, this resulted in a variable length control program, $\underline{u}(t)$. The result of this approach was an unsatisfactory computational process, since the terminal region of the control vectors could not be determined analytically when a change in the control program resulted in a flight profile whose time increased relative to the previous nominal profile. Increases in flight time usually were experienced when the optimizing program was making a large effort to improve the value of terminal conditions. Several techniques were tried in an effort to determine reasonable values of the control vectors in this undefined terminal region, but all were essentially unsatisfactory guesses which often resulted in making the terminal conditions worse. Consequently, an excessive amount of computation was required when trying to improve terminal conditions. This undesirable characteristic was eliminated by changing the independent variable to distance, s. Presented below are the system equations and variables used in the formulation of the program using this new technique.

Control Variables, $\underline{u}$

$C_L$, Power

State Variables, $\underline{x}$

$V$, $\gamma$, $h$, $z$

Independent Variable

$s$

Matrix Notations

$$\underline{u}(s) = \begin{bmatrix} C_L \\ \\ \text{Power} \end{bmatrix} , \qquad m = 2$$

$$\underline{x}(s) = \begin{bmatrix} V(s) \\ \gamma(s) \\ h(s) \\ z(s) \end{bmatrix} , \qquad n = 4$$

$$\underline{f}(s) = \begin{bmatrix} f_1 \\ f_2 \\ f_3 \\ f_4 \end{bmatrix} , \qquad n = 4$$

$$\underline{\Psi} = \begin{bmatrix} \Psi_1 \\ \Psi_2 \\ \Psi_3 \end{bmatrix} , \qquad p = 3$$

System Differential Equations

$$f_1 = \frac{dV}{ds} = \frac{1}{V\cos\gamma}\left[\frac{T-D}{m} - g\sin\gamma\right]$$

$$f_2 = \frac{d\gamma}{ds} = \left[\frac{L}{m\cos\gamma} - g\right]\frac{1}{V^2}$$

$$f_3 = \frac{dh}{ds} = \tan\gamma$$

$$f_4 = \frac{dz}{ds} = \frac{1}{V\cos\gamma}[a + bQ]$$

In addition, time of flight and fuel burned can be determined by

$$\frac{dt}{ds} = \frac{1}{V\cos\gamma}$$

$$\frac{dFUEL}{ds} = \frac{Q}{V\cos\gamma}$$

Performance Index

$$\Phi = z(s_f)$$

Terminal Constraints

$$\Psi_1 = V(s_f) - V^* = 0$$

$$\Psi_2 = \gamma(s_f) - \gamma^* = 0$$

$$\Psi_3 = h(s_f) - h^* = 0$$

where $(\ )^*$ are the specified terminal conditions as discussed in Section 2.1 and reviewed below.

$$V^* = 160 \text{ fps.}$$

$$\gamma^* = 0 \text{ radians}$$

$$h^* = 3500 \text{ feet}$$

The initial conditions had the same value as the terminal conditions.

Stopping Condition

$$\Omega = s_f - s^* = 0$$

where

$$s^* = 264{,}000 \text{ feet} = 50 \text{ miles}$$

Calculation of $\underline{F}$ matrix

The $\underline{F}$ matrix, defined by equation (A.2.4) is evaluated as follows

$$\underline{F} = \begin{bmatrix} \frac{\partial f_1}{\partial x_1}, & \cdots, & \frac{\partial f_1}{\partial x_4} \\ \cdot & & \cdot \\ \cdot & & \cdot \\ \cdot & & \cdot \\ \frac{\partial f_4}{\partial x_1}, & \cdots, & \frac{\partial f_4}{\partial x_4} \end{bmatrix}$$

where

$$\frac{\partial f_1}{\partial x_1} = \frac{\partial f_1}{\partial V} = \frac{1}{V^2 \cos\gamma} \left[ g \sin\gamma - \frac{2T+D}{m} \right]$$

$$\frac{\partial f_1}{\partial x_2} = \frac{\partial f_1}{\partial \gamma} = \frac{1}{V \cos^2\gamma} \left[ \frac{T-D}{m} \sin\gamma - g \right]$$

$$\frac{\partial f_1}{\partial x_3} = \frac{\partial f_1}{\partial h} = \frac{1}{mV\cos\gamma} \left[ \frac{\partial T}{\partial h} - \frac{\partial D}{\partial h} \right]$$

$$\frac{\partial f_1}{\partial x_4} = \frac{\partial f_1}{\partial z} = 0$$

$$\frac{\partial f_2}{\partial x_1} = \frac{\partial f_2}{\partial V} = \frac{2g}{V^3}$$

$$\frac{\partial f_2}{\partial x_2} = \frac{\partial f_2}{\partial \gamma} = \frac{L \tan\gamma}{mV^2 \cos\gamma}$$

$$\frac{\partial f_2}{\partial x_3} = \frac{\partial f_2}{\partial h} = \frac{1}{mV^2 \cos\gamma} \quad \frac{\partial L}{\partial h}$$

$$\frac{\partial f_2}{\partial x_4} = \frac{\partial f_2}{\partial z} = 0$$

$$\frac{\partial f_3}{\partial x_1} = \frac{\partial f_3}{\partial V} = 0$$

$$\frac{\partial f_3}{\partial x_2} = \frac{\partial f_3}{\partial \gamma} = \sec^2\gamma$$

$$\frac{\partial f_3}{\partial x_3} = \frac{\partial f_3}{\partial h} = 0$$

$$\frac{\partial f_3}{\partial x_4} = \frac{\partial f_3}{\partial z} = 0$$

$$\frac{\partial f_4}{\partial x_1} = \frac{\partial f_4}{\partial V} = - \frac{a + b\,Q}{V^2 \cos\gamma}$$

$$\frac{\partial f_4}{\partial x_2} = \frac{\partial f_4}{\partial \gamma} = \frac{(a+bQ)\ \tan\gamma}{V\cos\gamma}$$

$$\frac{\partial f_4}{\partial x_3} = \frac{\partial f_4}{\partial h} = \frac{b}{V\cos\gamma} \quad \frac{Q}{(h - \frac{30,000}{.55})}$$

$$\frac{\partial f_4}{\partial x_4} = \frac{\partial f_4}{\partial z} = 0$$

Calculation of $\underline{G}$ Matrix

The $\underline{G}$ matrix, defined by equation A.2.5, is evaluated as follows

$$\underline{G} = \begin{bmatrix} \frac{\partial f_1}{\partial u_1} & \frac{\partial f_1}{\partial u_2} \\ \vdots & \vdots \\ \frac{\partial f_4}{\partial u_1} & \frac{\partial f_4}{\partial u_2} \end{bmatrix}$$

where

$$\frac{\partial f_1}{\partial u_1} = \frac{\partial f_1}{\partial C_L} = - \frac{1}{mV\cos\gamma} \frac{2L}{\pi e(AR)}$$

$$\frac{\partial f_1}{\partial u_2} = \frac{\partial f_1}{\partial Power} = \frac{1}{mV\cos\gamma} \frac{T}{Power}$$

$$\frac{\partial f_2}{\partial u_1} = \frac{\partial f_2}{\partial C_L} = \frac{\rho(WAR)}{2m\cos\gamma}$$

$$\frac{\partial f_2}{\partial u_2} = \frac{\partial f_2}{\partial Power} = 0$$

$$\frac{\partial f_3}{\partial u_1} = \frac{\partial f_3}{\partial C_L} = 0$$

$$\frac{\partial f_3}{\partial u_2} = \frac{\partial f_2}{\partial Power} = 0$$

$$\frac{\partial f_4}{\partial u_1} = \frac{\partial f_4}{\partial C_L} = 0$$

$$\frac{\partial f_4}{\partial u_2} = \frac{\partial f_4}{\partial \text{Power}} = .64 \quad \frac{b}{V\cos\gamma} \; \frac{Q}{\text{Power}}$$

It is observed that as Power approaches zero, the value $\partial f_4/\partial u_2$ approaches infinity and the problem becomes insolvable. This would be the case if the minimum power constraint boundary were equal to zero. Fortunately, this constraint boundary was set to 10% of NRP as determined from physical considerations.

Terminal Values of $\underline{\lambda}$

$$\underline{\lambda}_\Phi^T(s_f) = \left[ \frac{\partial \Phi}{\partial V}, \; \frac{\partial \Phi}{\partial \gamma}, \; \frac{\partial \Phi}{\partial h}, \; \frac{\partial \Phi}{\partial z} \right]_{s=s_f}$$

$$= [0, 0, 0, 1]$$

$$\underline{\lambda}_\Psi^T(s_f) = \begin{bmatrix} \frac{\partial \Psi_1}{\partial x_1} & \cdots & \frac{\partial \Psi_1}{\partial x_4} \\ \vdots & & \vdots \\ \frac{\partial \Psi_3}{\partial x_1} & \cdots & \frac{\partial \Psi_3}{\partial x_4} \end{bmatrix}_{s=s_f}$$

$$= \begin{bmatrix} 1, & 0, & 0, & 0 \\ 0, & 1, & 0, & 0 \\ 0, & 0, & 1, & 0 \end{bmatrix}$$

$$\underline{\lambda}_{\Omega}^{T}(s_f) = \left[\frac{\partial\Omega}{\partial V}, \frac{\partial\Omega}{\partial\gamma}, \frac{\partial\Omega}{\partial h}, \frac{\partial\Omega}{\partial z}\right]_{s=s_f}$$

$$= [0,\ 0,\ 0,\ 0]$$

<u>Other terms</u>

Several other terms are needed for the solution of the optimal profile. These are presented below

$$\frac{d\Phi}{ds} = \left(\frac{dz}{ds}\right)_{s=s_f}$$

$$\frac{d\underline{\Psi}}{ds} = \begin{bmatrix} \frac{d\Psi_1}{ds} \\ \frac{d\Psi_2}{ds} \\ \frac{d\Psi_3}{ds} \end{bmatrix} = \begin{bmatrix} \frac{dV}{ds} \\ \frac{d\gamma}{ds} \\ \frac{dh}{ds} \end{bmatrix}$$

$$\frac{d\Omega}{ds} = 1$$

$$\underline{\lambda}_{\Phi\Omega} = \begin{bmatrix} \lambda_{\Phi_1} \\ \lambda_{\Phi_2} \\ \lambda_{\Phi_3} \\ \lambda_{\Phi_4} \end{bmatrix} - \frac{d\Phi}{ds} \times \begin{bmatrix} \lambda_{\Omega_1} \\ \lambda_{\Omega_2} \\ \lambda_{\Omega_3} \\ \lambda_{\Omega_4} \end{bmatrix}$$

$$\underline{\lambda}_{\Psi\Omega} = \begin{bmatrix} \lambda_{\Psi_{11}} & \cdots & \lambda_{\Psi_{13}} \\ \vdots & & \vdots \\ \lambda_{\Psi_{41}} & \cdots & \lambda_{\Psi_{43}} \end{bmatrix} - \begin{bmatrix} \lambda_{\Omega_1} \\ \vdots \\ \lambda_{\Omega_4} \end{bmatrix} \left[ \frac{d\Psi_1}{ds}, \frac{d\Psi_2}{ds}, \frac{d\Psi_3}{ds} \right]$$

## Auxiliary Equations

Auxiliary equations needed for completion of the system equations are presented below. The aircraft lift and drag are formulated as

$$L = \frac{1}{2} \rho V^2 \; C_L(WAR)$$

$$D = \frac{1}{2} \rho V^2 \; C_D(WAR)$$

where the drag coefficient is a function of profile and induced drag as

$$C_D = C_{D_o} + C_{D_i}$$

$$C_{D_i} = \frac{C_L^{\,2}}{\pi e(AR)}$$

Also needed are

$$\frac{\partial L}{\partial h} = \frac{1}{2} V^2 \; C_L(WAR) \; \frac{\partial \rho}{\partial h}$$

$$\frac{\partial D}{\partial h} = \frac{1}{2} V^2 \; C_D(WAR) \; \frac{\partial \rho}{\partial h}$$

The atmospheric density, $\rho$, is determined by

$$\rho = .002377(1 - .6875 \times 10^{-5}h)^{4.2561}$$

which is a model of the ICAO standard atmosphere ranging from 0 to 36,000 feet. The rate of change of density with altitude is easily determined to be

$$\frac{\partial \rho}{\partial h} = - \frac{.2926 \times 10^{-4}\rho}{1- .6875 \times 10^{-5}h}$$

Standard atmospheric temperatures have been assumed. As defined in Section 2.1, fuel flow rate and thrust are

$$Q = \frac{SFC_o}{3600} (\text{Power})^{.64}(\text{NRP})^{.36}(1 - \frac{.55h}{30,000})$$

$$T = \frac{550(\text{Power})\ \eta(1 - \frac{.55h}{30,000})}{V}$$

It can be easily determined that

$$\frac{\partial T}{\partial h} = \frac{T}{h - \frac{30,000}{.55}}$$

<u>Control Variable Inequality Constraints</u>

As described in Section 2.1 there are inequality constraints in both control variables. These are summarized below. The value of $C_{L_{min}}$ is arbitrary.

$C_{L_{max}} = 3.0$

$C_{L_{min}} = 0.0$

$Power_{max} = 18,800$

$Power_{min} = 1,880$

Formulating the control variable inequality constraints according to equation 2.3.1 results in

$$C_1 = (C_L - C_{L_{min}})(C_L - C_{L_{max}}) \leq 0$$

$$C_2 = (Power-Power_{min})(Power-Power_{max}) \leq 0$$

When either of the control variables are on the constraint boundary, the adjoint equation is modified by the addition of $\underline{\Delta F}$ as

$$\dot{\underline{\lambda}} = -[\underline{F} - \underline{\Delta F}]^T \underline{\lambda}$$

where

$$\underline{\Delta F} = \frac{\partial \underline{\underline{f}}}{\partial u} \left(\frac{\partial C}{\partial u}\right)^{-1} \frac{\partial C}{\partial \underline{x}}$$

A discussion of these equations has been presented in Section A.3 of Appendix A.

However, because the inequality constraints of this problem do not involve state variables, $\underline{\Delta F}$ equals zero and no change in the form of the adjoint equations is ever needed.

# CHAPTER III

## RESULTS AND CONCLUSIONS

The optimum profile and control history for a fifty mile flight of the commercial tilt wing VTOL aircraft is presented in Figures 4 through 8. Given that the lift coefficient and power were controlled as indicated in Figures 7 and 8, the optimal profile presented would result in a minimum value of the performance index of 30.54 dollars. This value is considerably smaller than the 84.48 dollars calculated for the initial steady state profile.

Since the aircraft is assumed to be flying at steady state conditions before and after the optimized flight region, the magnitude of the variables for these steady state conditions are shown on each plot. To make the plots easier to read, the abscissa scale in Figures 6 and 7 are expanded at the low and high values of distance.

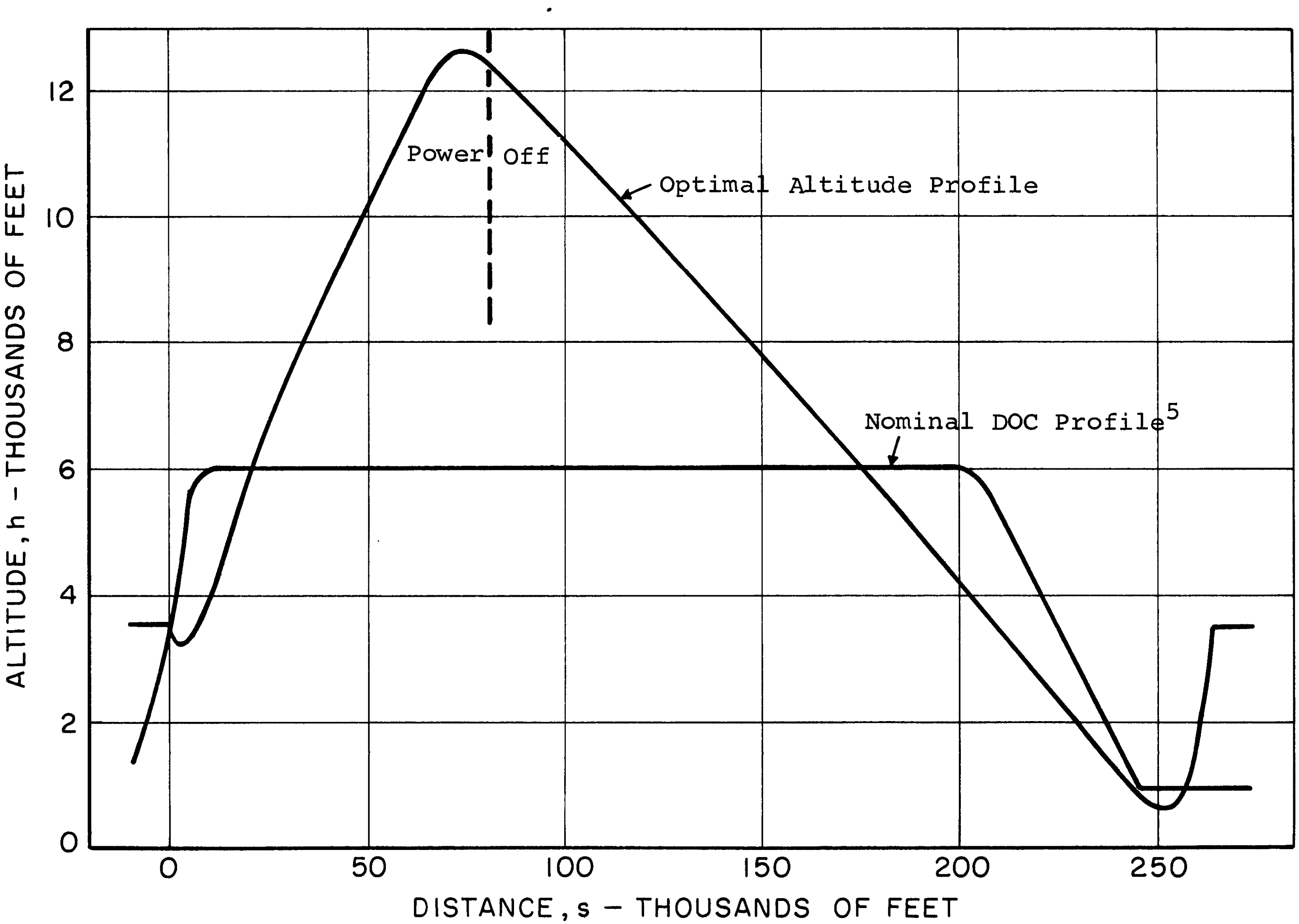


Figure 4. Optimum Altitude Profile

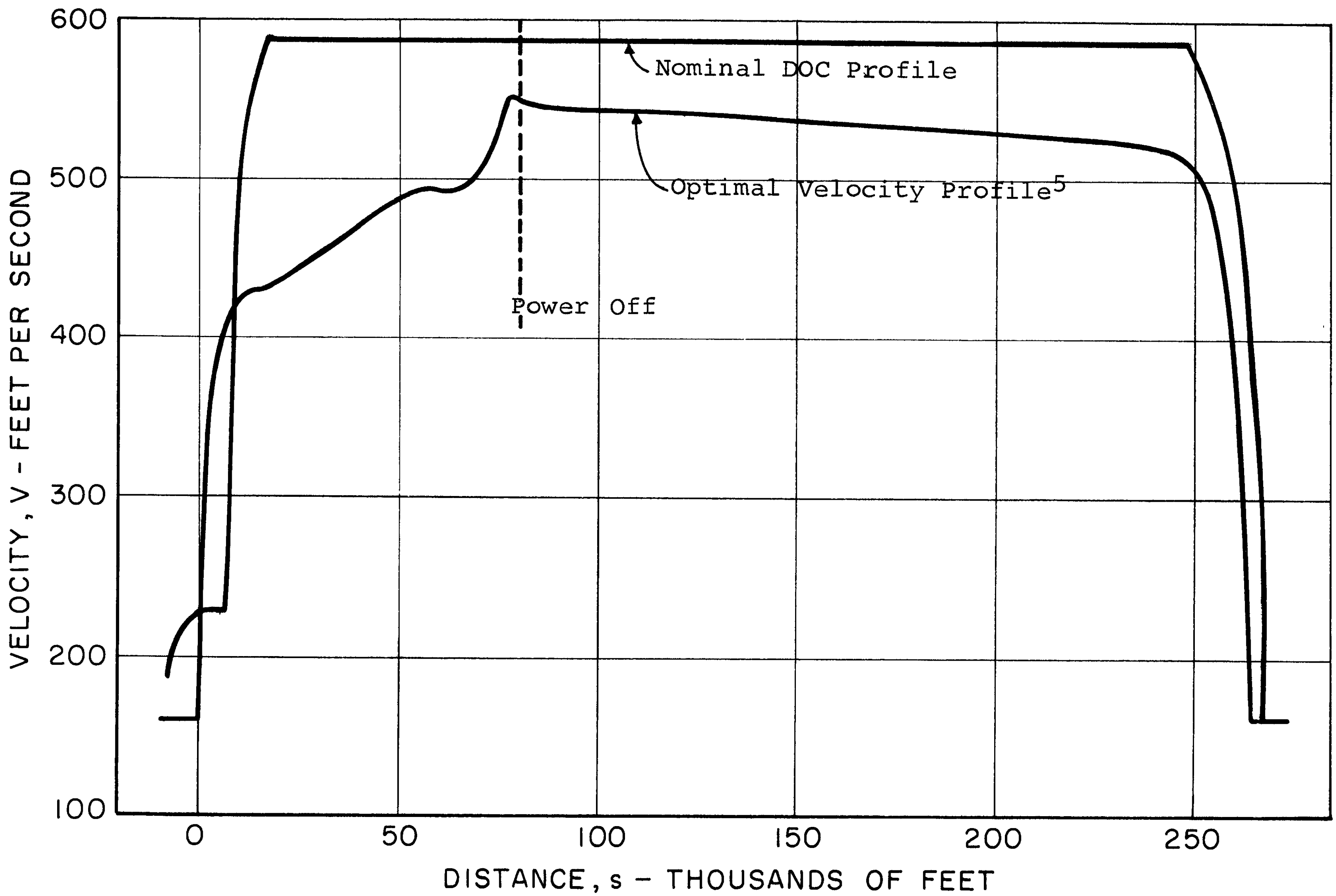


Figure 5. Optimum Velocity Profile

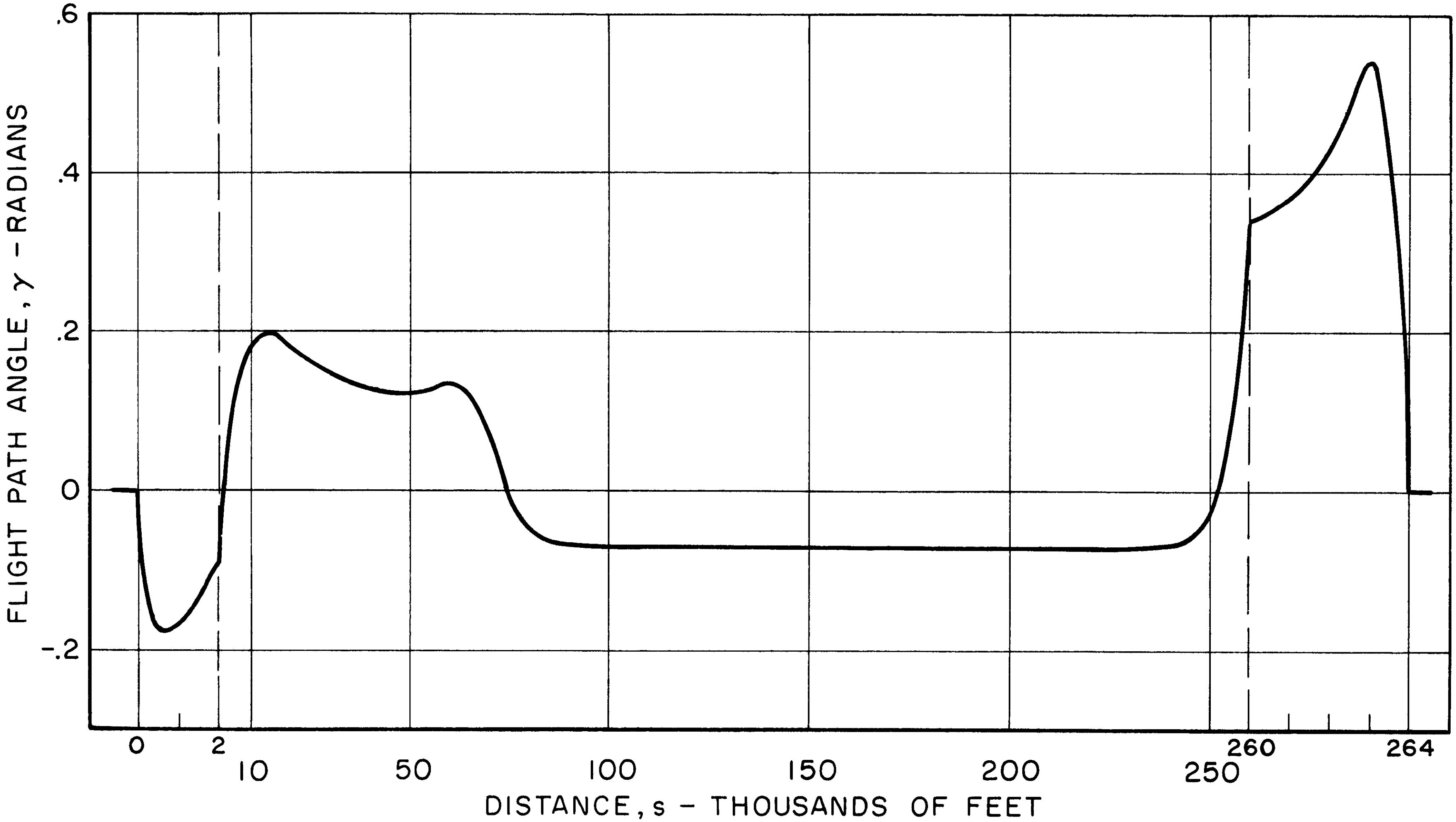


Figure 6. Optimum Flight Path Angle Profile

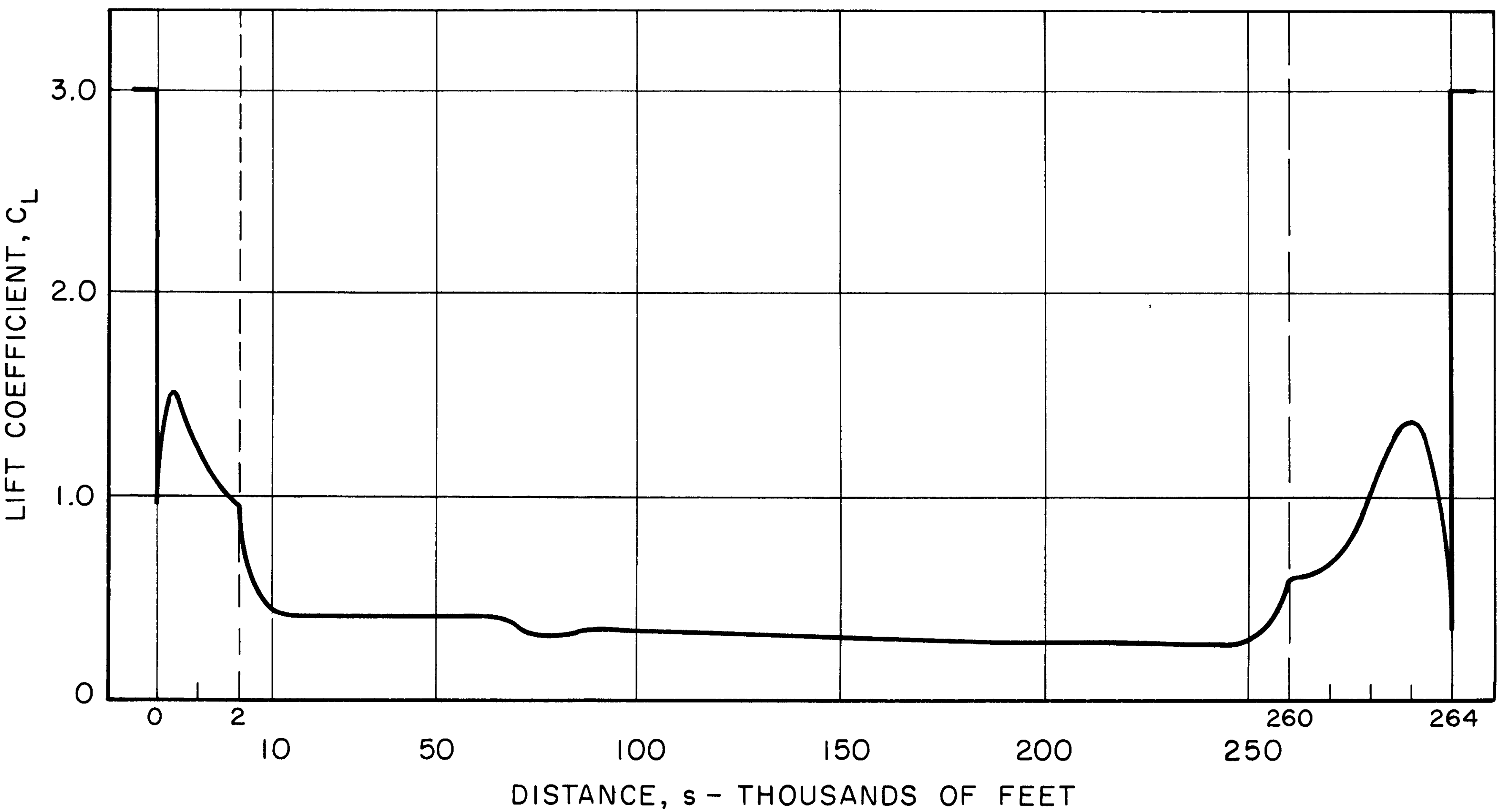


Figure 7. Optimum Lift Coefficient Control Program

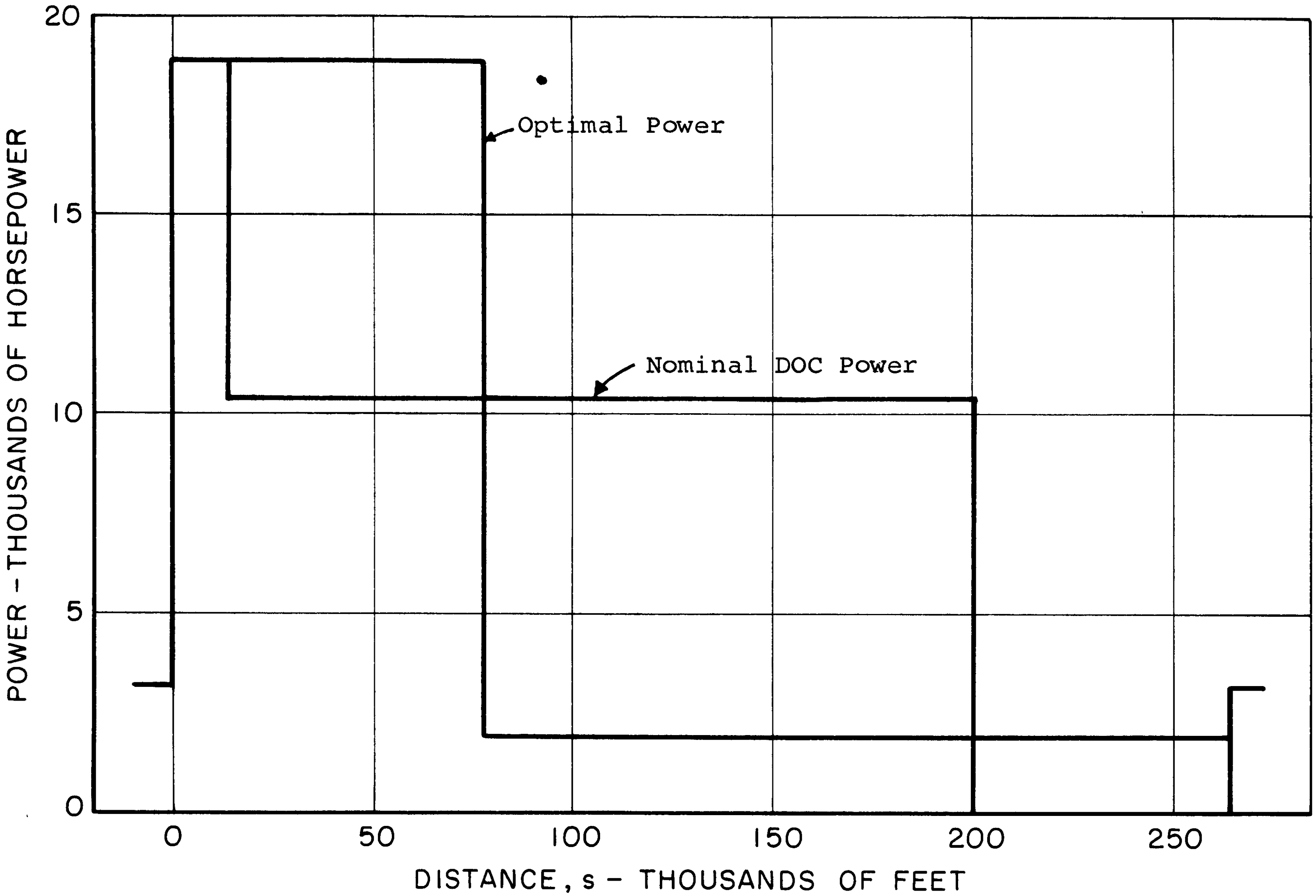


Figure 8. Optimum Power Control Program

The time cost is the major component of the DOC as is shown below.

| | DOC | Time Cost % DOC | Fuel Cost % DOC |
|---|---|---|---|
| Initial Steady State Profile | 84.48 | 70.7% | 29.3% |
| Optimum Profile | 30.54 | 63.6% | 36.4% |
| DOC Profile[5] | 31.60 | 57.2 | 42.8 |

Therefore, an intuitive conclusion would be that the aircraft would want to accelerate rapidly to a high velocity so as to minimize the time of flight. It is observed from the plots that this indeed does happen. To accomplish the high acceleration, Power is set at its maximum level at the beginning of the flight. The lift coefficient, $C_L$, is also rapidly reduced since this also contributes to acceleration of the aircraft and does so in two ways. First, the reduction of $C_L$ greatly reduces the induced drag coefficient and, therefore, allows the aircraft to accelerate faster than it otherwise would. The reduced $C_L$ also allows the aircraft to drop in altitude which in turn provides additional acceleration due to gravity. The reason for the peaking of $C_L$ at the beginning of the profile is not clear. The peaking at the terminal phase of the flight profile is apparently required to guide the aircraft to the specified terminal conditions.

It is also observed that the aircraft climbs to a relatively high altitude to take advantage of less dense air which results in lower drag and, therefore, less total power required. Apparently, the penalty of climbing to this high altitude is more than compensated for by the minimum power glide that follows. In fact, a second advantage of climbing to a high altitude is the resultant capability of then reducing power to a minimum. The fuel cost is then a minimum for the later half of the flight while high velocity is still maintained by the minimum power glide. The maximum altitude attained was 12,625 feet.

Since it is important from the time cost point of view that a high velocity be maintained for as long as possible, the aircraft flies below the terminal altitude as it approaches the terminal conditions and then dissipates its high kinetic energy by climbing very rapidly. The minimum altitude attained was 636 feet. It can be seen from Figure 5 that the true airspeed decreases slightly during descent, although the equivalent airspeed is increasing ($C_L$ decreases slightly in descent). The peak velocity over the profile was 551 feet per second while the average velocity was 492 feet per second.

A comparison of this "optimal" profile and the nominal DOC profiles used in Refs. 5, 6 can now be made. Figure 4 shows that the aircraft would like to climb to over 12000 feet at full power, and then reduce the power for a high speed glide to destination. The nominal DOC profile climbed (at maximum rate of climb) to 6000 feet, and spent a considerable portion of the trip in the cruise made at partial power.

Interestingly, the optimal profile has the aircraft climb at a speed varying from 400-500 fps or 270-340 mph, and a rate of climb of around 3440 fpm which is quite comparable to present jet transports. The nominal profile used a speed of 154 mph to achieve a maximum rate of climb around 7000 fpm.

Although the nominal cruise speed of this vehicle is 400 mph, the speed maintained during the glide on the optimal profile is only about 90% of this value, and varies slightly during descent. The nominal profile descends at a higher speed and rate of descent, and apparently uses speed brakes to kill its speed in level flight as opposed to the zoom required by the system equations for the optimal profile.

The purpose of determining the optimal profile was to gain insight into the economics of flying future commercial short haul aircraft. The optimal profile and its associated control program presented do indeed clear up the question of how to fly the aircraft for minimum cost. The answer is that full power should be used in the initial stages of the trip in order to accelerate and climb. The climb should be made at a high speed well above the speed for maximum rate of climb or for minimum L/D ratio. At the point where an altitude and speed are reached such that a power off high speed glide can be made to reach the destination, power should be put to minimum fuel consumption. The high speed during glide should be maintained to the point where deceleration using full braking capabilities will return the aircraft to the desired transition speed. It would seem desirable that this type of aircraft be equipped with speed brakes to assist in this deceleration.

In essence these are the practical results of the application of this mathematical technique. Because of passenger comfort, and ATC difficulties, it is not likely that one would attempt to fly the optimal profile. Operating within these constraints now indicates that full power should be used to get as high as possible. The climb speed should be about twice that for maximum rate of climb, and if possible a high speed descent should be made with power off. The selection of profiles can now proceed on this basis for engineering design, while considerations can continue of improving the mathematical techniques to incorporate these types of restrictions. The comparison shows that on a dollar cost basis, the nominal DOC profile is very close to the optimal trip cost, even though the altitude, speed, and power profiles are quite different.

## The Mathematical Technique

Several questions can now be raised as to the shortcomings of the optimization technique used and what research could be performed in the future to improve its usefulness. For example, the $C_L$ control program shown in Figure 5 makes a step change coming from and going to the steady state flight conditions at the beginning and end of the optimized flight profile. Physically, of course, this is impossible. This step is due to the fact that the initial and final values of $C_L$ were allowed to seek an unconstrained optimal level rather than start at the value required for steady state value at the very beginning and end of the profile. A rate constraint on $C_L$ could also be applied to simulate the time lag in the control process.

Another undesirable feature of the profile is the fact that the aircraft goes below the terminal altitude by an unacceptable amount. To prevent this, linear and quadratic altitude penalty functions were attempted as part of the research for this report. They unfortunately resulted in computational instability and were discarded. The application of a state variable inequality constraint technique may work more successfully.

The application of inequality constraints on $C_L$ and Power to limit the normal and longitudinal accelerations that the passengers would encounter is another important contribution that could be made to the problem. It was determined, for example, that for this aircraft the passengers would be subjected to about .75 g's in the longitudinal direction at the beginning of the flight. This is too high for commercial operation. Similar acceleration perturbations were observed in the normal direction. It would be of valuable interest to determine how much the optimum DOC changes if all of the above constraints were introduced, as well as to determine the DOC penalty due to air traffic control constraints.

Significant improvements in the application of the calculus of variations to this problem is also important. The outstanding difficulty with the steepest descent method used was the extremely slow rate of convergence to the optimal. This is evidenced by the large amount of computing time necessary to solve the problem. Using the computational techniques that were found to perform best, approximately 150 control program iterations were required to reach the optimum from the original steady state nominal. Each iteration required about 2 minutes of IBM 7094 computing time, which amounts to approximately 5 hours of computation. This does not include the many hours of computing time used in developing a satisfactory approach to the solution of the problem. The extremely long computation required seems to be due to a very nonlinear function space created by the unusual performance index and the nonlinear equation for the fuel flow rate.

Significant improvements in the application of the technique must be made if we are to benefit from its theoretical capabilities. One possible approach to solving the above problem is to find a method to determine the best direction as well as step size of $\delta \underline{u}$ in function space which will maximize the reduction of the performance index in a stable fashion, as indicated in Appendix B. This might be accomplished by the proper control of the weighting factor, $\underline{W}$. Two other calculus of variations techniques that may be useful in the efficient solution of this problem are the conjugate gradient and the second order methods. Much more research is also required to gain a better understanding of the numerical solution of the steepest descent method and to develop better techniques to insure computational stability.

One of the major shortcomings of the solution of all optimal control problems requiring numerical solution is that the most efficient and successful techniques used are generally different for each type of problem. Much more research is needed to develop good numerical techniques and procedures that can be more universally applied.

# BIBLIOGRAPHY

1. ANALYSIS OF V/STOL AIRCRAFT CONFIGURATIONS FOR SHORT HAUL AIR TRANSPORTATION SYSTEMS, FT-66-1, November 1966, R. Gallant, W. Lange, M. Scully

2. MAINTENANCE COST STUDIES OF PRESENT AIRCRAFT SUBSYSTEMS, FT-66-2, November 1966, R.W. Simpson, C. Pearlman.

3. COMPUTERIZED SCHEDULE CONSTRUCTION FOR AN AIRLINE TRANSPORTATION SYSTEM, FT-66-3, November 1966, R.W. Simpson.

4. WEATHER CONDITIONS AFFECTING VTOL AIRBUS OPERATIONS IN THE NORTHEAST CORRIDOR, FT-66-4, November 1966, R.W. Simpson.

5. APPLICATION OF THE CALCULUS OF VARIATIONS IN DETERMINING OPTIMUM FLIGHT PROFILES FOR COMMERCIAL SHORT HAUL AIRCRAFT, FT-66-5, November 1966, R. Gallant

# REFERENCES

1. Bryson, A.E., Denham, W.F.,"A Steepest-Ascent Method for Solving Optimum Programming Problems"; Journal of Applied Mechanics, pp. 247-257, June, 1962.

2. Bryson, A.E., Denham, W.F., Dreyfus, S.E., "Optimal Programming Problems with Inequality Constraints, I: Necessary Conditions for External Solutions"; AIAA Journal, Vol. 1, No. 11, pp. 2544-2550, November, 1963.

3. Denham, W.F., Bryson, A.E., "Optimal Programming Problems with Inequality Constraints, II: Solution by Steepest-Ascent"; AIAA Journal, Vol. 2, No. 1, pp. 25-34, January, 1964.

4. Standard Method of Estimating Comparative Direct Operating Costs of Transport Airplanes; published by Air Transport Association of America, 1960.

5. Miller, R.H., et al.; "A Systems Analysis of Short Haul Air Transportation"; Flight Transportation Laboratory, Massachusetts Institute of Technology, August 1965. Sponsored by U.S. Department of Commerce, Contract No. C-85-65.

6. Gallant, R.A., Scully, M., Lange, W.; "Analysis of Aircraft Concepts for Short Haul Air Transportation Systems"; Flight Transportation Laboratory, Massachusetts Institute of Technology, November 1966. Sponsored by U.S. Department of Commerce, Contract No. C-136-66.

# NOMENCLATURE

| | |
|---|---|
| a | time cost coefficient of DOC, dollars/second. |
| AR | wing aspect ratio. |
| b | fuel cost coefficient of DOC, dollars/lb. of fuel. |
| C | generalized control variable inequality constraint. |
| $C_{D_O}$ | profile drag coefficient. |
| $C_L$ | lift coefficient. |
| D | drag, lbs. |
| $\underline{D}$ | $\underline{\lambda}_{\Phi\Omega}^T \underline{G}$ |
| DOC | direct operating cost, dollars. |
| dP | total change in $\delta\underline{u}$ |
| e | wing efficiency factor. |
| $\underline{E}$ | $\underline{\lambda}_{\underline{\Psi}\Omega}^T \underline{G}$ |
| f( ) | function of ( ) |
| FUEL | fuel consumed, lbs. |
| $\underline{F}$ | perturbation matrix of $\underline{x}$. |
| g | acceleration of gravity, ft/sec$^2$. |
| g( ) | function of ( ). |
| $\underline{G}$ | perturbation matrix of $\underline{u}$. |
| h | altitude, feet. |
| $\underline{I}_{\underline{\Psi\Psi}}$, $\underline{I}_{\underline{\Psi}\Phi}$, $I_{\Phi\Phi}$ | auxiliary integrals. |
| L | lift, lbs. |
| m | aircraft mass, slugs. |
| NRP | engine normal rated power, horsepower. |

| | |
|---|---|
| Power | engine power, horsepower. |
| Q | fuel flow rate, lbs/sec. |
| s | horizontal distance, feet. |
| SFC | specific fuel consumption. |
| $SFC_o$ | specific fuel consumption at NRP. |
| t | time, sec. |
| T | thrust, lb. |
| $\underline{u}$ | vector of control variables. |
| V | velocity, fps. |
| WAR | wing area, sq. ft. |
| $W_A$ | weight of airframe, lb. |
| $W_E$ | weight of engine, lb. |
| $W_{gr}$ | aircraft gross weight. |
| $\underline{W}$ | matrix weighting factor. |
| $\underline{x}$ | vector of state variables. |
| z | DOC, dollars. |
| $\gamma$ | flight path angle, radians. |
| $\delta$ | perturbation. |
| $\eta$ | propeller-transmission efficiency. |
| $\lambda$ | adjoint variable (influence function). |
| $\rho$ | air density, slugs/ft$^3$ |
| $\Phi$ | performance index. |
| $\underline{\Psi}$ | constraint on terminal conditions. |
| $\Omega$ | stopping condition. |
| $d\underline{\beta}$ | specified change in terminal conditions. |
| $d\underline{\Psi}$ | error in terminal conditions. |

Subscripts:

| | |
|---|---|
| $(\ )_o$ | initial conditions. |
| $(\ )_f$ | final conditions. |
| $(\ )_1$ | beginning of constraint boundary. |
| $(\ )_2$ | end of constraint boundary. |
| $(\underline{\ })$ | vector or matrix. |

Superscripts:

| | |
|---|---|
| $(\dot{\ })$ | time derivative. |
| $(\ )'$ | distance derivative. |
| $(\ )^*$ | specified terminal conditions. |
| $(\ )^T$ | matrix transpose. |
| $(\ )^{-1}$ | matrix inverse. |
| $(\bar{\ })$ | nominal program. |

# Appendix A

# OPTIMIZATION THEORY

## A.1 Nomenclature description

As a means to determining the optimal flight profile program, a convenient formulation of the calculus of variations problem which lends itself to digital computer solution is presented. An unspecified terminal time problem is considered and terminal constraints on some or all of the state variables is optional.

The basic objective is to determine the control vector time history $\underline{u}(t)$ in the interval $t_o \leq t \leq t_f$ which will maximize a performance index

$$\Phi = \Phi[\underline{x}(t_f),\ t_f] \qquad \text{(A.1.1)}$$

subject to three sets of constraints,

$$\dot{\underline{x}} = \underline{f} = \underline{f}[\underline{x}(t),\ \underline{u}(t),\ t] \qquad \text{(A.1.2)}$$

system differential equations, $t_o$ and $\underline{x}(t_o)$ given.

$$\underline{\Psi} = \underline{\Psi}[\underline{x}(t_f), t_f] = \underline{0} \tag{A.1.3}$$

terminal constraints.

$$\Omega = \Omega[\underline{x}(t_f), t_f] = 0 \tag{A.1.4}$$

stopping condition.

In contrast to a calculus of variations problem where a closed form solution is possible, the addition of $\underline{\Psi}$ and $\Omega$ constraints to the formulation is necessary when a digital computer step by step solution is to be employed. The $\underline{\Psi}$ constraints are necessary to satisfy the terminal boundary conditions while the $\Omega$ constraint simply specifies when integration operations have reached a desired stopping condition. The nomenclature for the above is:

$$\underline{u}(t) = \begin{bmatrix} u_1(t) \\ \cdot \\ \cdot \\ \cdot \\ u_m(t) \end{bmatrix} \tag{A.1.5}$$

an $m \times 1$ matrix of control variable programs which we are free to choose.

$$\underline{x}(t) = \begin{bmatrix} x_1(t) \\ \cdot \\ \cdot \\ \cdot \\ x_n(t) \end{bmatrix} \tag{A.1.6}$$

an $n \times 1$ matrix of state variables which result from the choice $\underline{u}(t)$ and $\underline{x}(t_o)$.

$$\underline{f} = \begin{bmatrix} f_1 \\ \cdot \\ \cdot \\ \cdot \\ f_n \end{bmatrix} = \begin{bmatrix} \dot{x}_1(t) \\ \cdot \\ \cdot \\ \cdot \\ \dot{x}_n(t) \end{bmatrix} \tag{A.1.7}$$

an $n \times 1$ matrix of known system differential equations of $\underline{x}(t)$ $\underline{u}(t)$ and $t$.

$$\underline{\Psi} = \begin{bmatrix} \Psi_1 \\ \cdot \\ \cdot \\ \cdot \\ \Psi_p \end{bmatrix} \tag{A.1.8}$$

a $p \times 1$ matrix of terminal constraints where $p \leq n$. Each is a known function of $\underline{x}(t_f)$ and $t_f$.

$\Phi$ is the performance index to be maximized and is a known function of $\underline{x}(t_f)$ and $t_f$.

$\Omega=0$ is the stopping condition which determines $t_f$ and is a known function of $\underline{x}(t_f)$ and $t_f$.

A steepest ascent method in the calculus of variations can now be derived to determine the control vector time history, $\underline{u}(t)$, which will satisfy the three sets of constraints and maximize the performance index, $\Phi$. A digital computer can be used to perform these repetitive operations. Basically, the technique starts with a nominal control program and determines the resultant history of the state variables by integrating from $\underline{x}(t_o)$ to the stopping condition, $\Omega = 0$. The control program is then improved, in a finite step by step fashion, in an attempt to converge on the specified constraints, as well as minimize $\Phi$. Improvement of the control program is accomplished by determining what effect local finite linear perturbations of $\underline{u}(t)$ (about its nominal value) has on the three sets of constraints. Appropriate finite changes in the control program are then made so as to approach the desired constraint relations. The process is repeated until all constraints are reasonably satisfied. The rigorous mathematics necessary to obtain an optimal control program efficiently is presented in the next section.

## A.2 Steepest Descent Method in the Calculus of Variations

Assuming that a nominal control program has been specified and the state variable time history determined, it is desired to make improvements in the control program. The objective is to satisfy the stated constraints, $\underline{\Psi}$ and $\Omega$, and minimize the performance index, $\Phi$. The technique of steepest descent, presented by Bryson[1], works well in this case. First, consider small linear perturbations, $\delta\underline{u}(t)$, about the nominal control program where

$$\delta\underline{u}(t) = \underline{u}(t) - \overline{\underline{u}}(t) \tag{A.2.1}$$

and $\overline{\underline{u}}(t)$ is the nominal program

$\underline{u}(t)$ is a change in the nominal program

These perturbations will cause perturbations in the state variables, $\delta\underline{x}(t)$, where

$$\delta\underline{x}(t) = \underline{x}(t) - \overline{\underline{x}}(t) \tag{A.2.2}$$

Substituting these relations into the differential equations (2.1.2) we obtain to first order in the perturbations.

$$\delta\dot{\underline{x}} = \underline{F}(t)\ \delta\underline{x} + \underline{G}(t)\delta\underline{u} \tag{A.2.3}$$

where

$$\underline{F} = \begin{bmatrix} \frac{\partial f_1}{\partial x_1} & \cdots & \frac{\partial f_1}{\partial x_n} \\ \vdots & & \vdots \\ \frac{\partial f_n}{\partial x_1} & \cdots & \frac{\partial f_n}{\partial x_n} \end{bmatrix}, \quad n \times n \text{ matrix} \tag{A.2.4}$$

$$\underline{G} = \begin{bmatrix} \frac{\partial f_1}{\partial u_1} & \cdots & \frac{\partial f_1}{\partial u_m} \\ \vdots & & \vdots \\ \frac{\partial f_n}{\partial u_1} & \cdots & \frac{\partial f_n}{\partial u_m} \end{bmatrix}, \quad n \times m \text{ matrix} \tag{A.2.5}$$

and where the partial derivatives are evaluated along the nominal path.

Now introduce the linear adjoint equations which are associated with equation (A.2.3)

$$\dot{\underline{\lambda}} = -\underline{F}^T(t)\underline{\lambda} \tag{A.2.6}$$

This equation applies to three sets of adjoint variables associated with the constraint functions, that is,

$$\underline{\lambda} = [\underline{\lambda}_\Phi, \underline{\lambda}_{\underline{\Psi}}, \underline{\lambda}_\Omega] \tag{A.2.7}$$

where

$$\underline{\lambda}_\Phi^T = [\lambda_{\Phi_1}, \ . \ . \ . \ , \lambda_{\Phi_n}] \tag{A.2.8}$$

$$\underline{\lambda}_{\underline{\Psi}}^T = \begin{bmatrix} \lambda_{\Psi_{11}}, & \cdots, & \lambda_{\Psi_{n1}} \\ \vdots & & \vdots \\ \lambda_{\Psi_{1p}}, & \cdots, & \lambda_{\Psi_{np}} \end{bmatrix} \tag{A.2.9}$$

$$\underline{\lambda}_\Omega^T = [\lambda_{\Omega_1}, \ . \ . \ . \ , \lambda_{\Omega_n}] \tag{A.2.10}$$

The important attributes of the λ's is that they are influence functions, i.e., they specify how much the terminal conditions will change with small changes in the state variables.

The terminal values of the adjoint variables are determined by

$$\underline{\lambda}_{\Phi}^{T}(t_f) = \left(\frac{\partial \Phi}{\partial \underline{x}}\right)_{t=t_f} = \left[\frac{\partial \Phi}{\partial x_1}, \ . \ . \ . \ , \frac{\partial \Phi}{\partial x_n}\right]_{t=t_f}, \qquad 1 \times n \text{ matrix} \tag{A.2.11}$$

$$\underline{\lambda}_{\underline{\Psi}}^{T}(t_f) = \left(\frac{\partial \underline{\Psi}}{\partial \underline{x}}\right)_{t=t_f} = \begin{bmatrix} \frac{\partial \Psi_1}{\partial x_1}, & . \ . \ ., & \frac{\partial \Psi_1}{\partial x_n} \\ \cdot & & \cdot \\ \cdot & & \cdot \\ \cdot & & \cdot \\ \frac{\partial \Psi_p}{\partial x_1}, & . \ . \ ., & \frac{\partial \Psi_1}{\partial x_n} \end{bmatrix}_{t=t_f}, \qquad p \times n \text{ matrix} \tag{A.2.12}$$

$$\underline{\lambda}_{\Omega}^{T}(t_f) = \left(\frac{\partial \Omega}{\partial \underline{x}}\right)_{t=t_f} = \left[\frac{\partial \Omega}{\partial x_1}, \ . \ . \ . \ , \frac{\partial \Omega}{\partial x_n}\right]_{t=t_f}, \qquad 1 \times n \text{ matrix} \tag{A.2.13}$$

The terminal values of the adjoint variable, $\underline{\lambda}(t_f)$, are evaluated for the nominal path. The value of $\underline{\lambda}(t)$ along the path can be obtained by integrating backwards from the terminal value. The adjoint variables may now be used to determine the changes in $\Phi$, $\underline{\Psi}$, and $\Omega$ due to small changes in the control program, the initial condition, $\delta\underline{x}(t_o)$, and terminal time, $dt_f$, by applying the following relationships.

$$d\Phi = \int_{t_o}^{t_f} \underline{\lambda}_{\Phi}^{T}(t)\underline{G}(t)\delta\underline{u}(t)dt + \underline{\lambda}_{\Phi}^{T}(t_o)\delta\underline{x}(t_o) + \dot{\Phi}dt_f \qquad (A.2.14)$$

$$d\underline{\Psi} = \int_{t_o}^{t_f} \underline{\lambda}_{\Psi}^{T}(t)\underline{G}(t)\delta\underline{u}(t)dt + \underline{\lambda}_{\Psi}^{T}(t_o)\delta\underline{x}(t_o) + \dot{\underline{\Psi}}dt_f \qquad (A.2.15)$$

$$d\Omega = \int_{t_o}^{t_f} \underline{\lambda}_{\Omega}^{T}(t)\underline{G}(t)\delta\underline{u}(t)dt + \underline{\lambda}_{\Omega}^{T}(t_o)\delta\underline{x}(t_o) + \dot{\Omega}dt_f \qquad (A.2.16)$$

where $\dot{\Phi}$, $\dot{\underline{\Psi}}$ and $\dot{\Omega}$ are defined on the nominal path as

$$\dot{\Phi} = \left(\frac{\partial\Phi}{\partial t} + \frac{\partial\Phi}{\partial\underline{x}}\underline{f}\right)_{t=t_f} \qquad (A.2.17)$$

$$\dot{\underline{\Psi}} = \left(\frac{\partial\underline{\Psi}}{\partial t} + \frac{\partial\underline{\Psi}}{\partial\underline{x}}\underline{f}\right)_{t=t_f} \qquad (A.2.18)$$

$$\dot{\Omega} = \left(\frac{\partial\Omega}{\partial t} + \frac{\partial\Omega}{\partial\underline{x}}\underline{f}\right)_{t=t_f} \qquad (A.2.19)$$

The value of $\delta \underline{x}(t_o)$ will be taken to be zero for this formulation since the initial time is considered to be fixed.

We now add an additional scalar constraint, $(dP)^2$, whose function is to specify the "total accumulated change" in the control program over the interval $t_o \leq t \leq t_f$ and is defined as

$$(dP)^2 = \int_{t_o}^{t_f} \delta \underline{u}^T(t)\ \underline{W}(t) \delta \underline{u}(t) dt \qquad (A.2.20)$$

where $\underline{W}(t)$ is an arbitrary $m \times m$ matrix of weighting functions which are used to adjust the relative magnitude of the elements of $\delta \underline{u}(t)$. It can also be used to decrease the magnitude of $\delta \underline{u}(t)$ in certain sensitive regions of the trajectory, if necessary. With this constraint, a small value of dP may now be arbitrarily chosen which will sufficiently insure small perturbations of $\delta \underline{u}(t)$, the result being that the linearity assumed in the development of the steepest descent equations will be reasonably valid. The magnitude of dP which will sufficiently insure linearity seems best determined by experience in operating the optimization program on the computer.

The proper choice of $\delta \underline{u}(t)$ which will minimize the performance index and satisfy the terminal constraints can be shown to be

$$\delta\underline{u}(t) = \pm\, \underline{W}^{-1}\underline{G}^T(\underline{\lambda}_{\Phi\Omega} - \underline{\lambda}_{\Psi\Omega}\underline{\underline{I}}_{\Psi\Psi}^{-1}\underline{I}_{\Psi\Phi}) \left[\frac{(dP)^2 - d\underline{\beta}^T\underline{\underline{I}}_{\Psi\Psi}^{-1}d\underline{\beta}}{I_{\Phi\Phi} - \underline{I}_{\Psi\Phi}^T\underline{\underline{I}}_{\Psi\Psi}^{-1}\underline{I}_{\Psi\Phi}}\right]^{\frac{1}{2}}$$

$$+\, \underline{W}^{-1}\,\underline{G}^T\underline{\lambda}_{\Psi\Omega}\underline{\underline{I}}_{\Psi\Psi}^{-1}d\underline{\beta} \quad m \times 1 \text{ matrix} \tag{A.2.21}$$

where

$$d\underline{\beta} = d\underline{\Psi} - \underline{\lambda}_{\Psi\Omega}^T(t_o)\,\delta\underline{x}(t_o) \qquad p \times 1 \text{ matrix} \tag{A.2.22}$$

$$\underline{\lambda}_{\Phi\Omega} = \underline{\lambda}_{\Phi} - \frac{\dot{\Phi}}{\dot{\Omega}}\,\underline{\lambda}_{\Omega} \qquad n \times 1 \text{ matrix} \tag{A.2.23}$$

$$\underline{\lambda}_{\Psi\Omega} = \underline{\lambda}_{\Psi} - \underline{\lambda}_{\Omega}\,\frac{\dot{\underline{\Psi}}^T}{\dot{\Omega}} \qquad n \times p \text{ matrix} \tag{A.2.24}$$

$$\underline{\underline{I}}_{\Psi\Psi} = \int_{t_o}^{t_f} \underline{\lambda}_{\Psi\Omega}^T\underline{G}\,\underline{W}^{-1}\underline{G}^T\underline{\lambda}_{\Psi\Omega}dt \qquad p \times p \text{ matrix} \tag{A.2.25}$$

$$\underline{\underline{I}}_{\Psi\Psi}(t_o) = \underline{0}$$

$$\underline{I}_{\Psi\Phi} = \int_{t_o}^{t_f} \underline{\lambda}_{\Psi\Omega}^T\underline{G}\,\underline{W}^{-1}\underline{G}^T\underline{\lambda}_{\Phi\Omega}\,dt \qquad p \times 1 \text{ matrix} \tag{A.2.26}$$

$$\underline{I}_{\Psi\Phi}(t_o) = \underline{0}$$

$$I_{\Phi\Phi} = \int_{t_o}^{t_f} \underline{\lambda}_{\Phi\Omega}^T\underline{G}\,\underline{W}^{-1}\underline{G}^T\underline{\lambda}_{\Phi\Omega}\,dt \qquad 1 \times 1 \text{ matrix} \tag{A.2.27}$$

$$I_{\Phi\Phi}(t_o) = 0$$

Observing the formulation of equation (A.2.22) it is clear that the second term of the right hand side is zero for the problem being considered since $\underline{x}(t_o)$ is fixed. Note also that the numerator in the square root of equation (A.2.21) can become negative for large values of $d\underline{\beta}$, thus there is a limit to the magnitude of $d\underline{\beta}$ for a given value of dP. A positive sign is used in front of equation (A.2.21) if the performance index is to be maximized, a negative sign if it is to be minimized. The predicted change in $\Phi$ for a change in the control program, equation (A.2.21) is

$$d\Phi = \pm[(dP^2 - d\underline{\beta}^T \underline{\underline{I}}_{\Psi\Psi}^{-1} d\underline{\beta})(I_{\Phi\Phi} - \underline{I}_{\Psi\Phi}^T \underline{\underline{I}}_{\Psi\Psi}^{-1} \underline{I}_{\Psi\Phi})]^{\frac{1}{2}}$$

$$+ \underline{I}_{\Psi\Phi}^T \underline{\underline{I}}_{\Psi\Psi}^{-1} d\underline{\beta} + \underline{\lambda}_{\Phi\Omega}^T (t_o) \delta\underline{x}(t_o) \qquad \text{(A.2.28)}$$

If $\underline{x}(t_o)$ is fixed (as in this problem) and the terminal constraints are satisfied, $\underline{\Psi} = \underline{0}$, then equation (A.2.28) can be reduced to

$$\frac{d\Phi}{dP} = \pm(I_{\Phi\Phi} - \underline{I}_{\Psi\Phi}^T \underline{\underline{I}}_{\Psi\Psi}^{-1} \underline{I}_{\Psi\Phi})^{\frac{1}{2}} \qquad \text{(A.2.29)}$$

which is the gradient of the performance index with respect to dP. As the optimal program is approached, this gradient will tend to zero. Using the change in the control program, $\delta\underline{u}(t)$, determined by equation (A.2.21) an improvement of the nominal program can be made by specifying a new control time history as

$$\underline{u}(t)_{new} = \underline{u}(t)_{old} + \delta\underline{u}(t) \qquad (A.2.30)$$

The new control program is then used in the new system differential equations (A.1.2). The whole optimization process is repeated until the terminal constraints are satisfied, $\underline{\Psi} = \underline{0}$, and the gradient (A.2.29) is very small.

## A.3 Control Variable Inequality Constraints

For the optimization problem being considered inequality constraints on the control variables are required if the results are to be of practical value. The essentials of a technique to accomplish this requirement are presented below[2,3].

Consider a control inequality constraint of the form

$$C[\underline{x}(t),\ u(t),\ t] \leq 0 \qquad (A.3.1)$$

where C is a scalar function, u(t) is a scalar control variable, and $\frac{\partial C}{\partial u} \neq 0$ for all u. Only a scalar quantity is considered for simplicity of presentation. The solution of optimal control problems with inequality constraints on the control variable is calculated in the same manner as the previously described unconstrained system except in the constraint boundary region. The adjoint equations necessary for determining an optimal solution with a control constraint are

$$\dot{\underline{\lambda}} = -\underline{F}^T(t)\underline{\lambda}$$ when $C < 0$, i.e., the system is off the constraint boundary (A.3.2)

$$\dot{\underline{\lambda}} = -[\underline{F}(t) - \underline{\Delta F}(t)]^T\underline{\lambda}$$ when $C = 0$, i.e., the system is on the constraint boundary (A.3.3)

where

$$\underline{\Delta F} = \frac{\partial \underline{f}}{\partial u}\left(\frac{\partial C}{\partial u}\right)^{-1}\frac{\partial C}{\partial \underline{x}} \qquad n \times n \text{ matrix} \tag{A.3.4}$$

$$\frac{\partial \underline{f}}{\partial C} = \begin{bmatrix} \frac{\partial f_1}{\partial C} \\ \cdot \\ \cdot \\ \cdot \\ \frac{\partial f_n}{\partial C} \end{bmatrix} \qquad n \times 1 \text{ matrix} \tag{A.3.5}$$

$$\frac{\partial C}{\partial \underline{x}} = \begin{bmatrix} \frac{\partial C}{\partial x_1}, & . & . & . & , \frac{\partial C}{\partial x_n} \end{bmatrix} \qquad 1 \times n \text{ matrix} \tag{A.3.6}$$

Also, $C(\underline{x}(t), u(t), t) = 0$ determines $u(t)$ when $C = 0$, otherwise, $u(t)$ is determined by the change in the nominal control program as follows

$$\delta u(t) = \pm W^{-1} \left[\frac{\partial \underline{f}}{\partial u}\right]^T (\underline{\lambda}_{\Phi\Omega} - \underline{\lambda}_{\Psi\Omega}\underline{\underline{I}}_{\Psi\Psi}^{-1}\underline{I}_{\Psi\Phi}) \left[\frac{(dP)^2 - d\underline{\beta}^T\underline{\underline{I}}_{\Psi\Psi}^{-1}d\underline{\beta}}{I_{\Phi\Phi} - \underline{I}_{\Psi\Phi}\underline{\underline{I}}_{\Psi\Psi}^{-1}\underline{I}_{\Psi\Phi}}\right]^{\frac{1}{2}}$$

$$+ W^{-1} \left[\frac{\partial \underline{f}}{\partial u}\right]^T \underline{\lambda}_{\Psi\Omega}\underline{\underline{I}}_{\Psi\Psi}^{-1} d\underline{\beta}\,, \qquad \begin{array}{l} t \leq t_1 \\ t \geq t_2 \end{array} \qquad \text{(A.3.7)}$$

where $t_1$ and $t_2$ are the initial and terminal states of the region where $u(t)$ is on the inequality constraint boundary, $C = 0$. Also

$$\underline{\underline{I}}_{\Psi\Psi} = \int_{t_o}^{t_1} + \int_{t_2}^{t_f} \underline{\lambda}_{\Psi\Omega}^T \frac{\partial \underline{\underline{f}}}{\partial u} W^{-1} \left(\frac{\partial \underline{\underline{f}}}{\partial u}\right)^T \underline{\lambda}_{\Psi\Omega} dt \qquad \text{(A.3.8)}$$

$$\underline{I}_{\Psi\Phi} = \int_{t_o}^{t_1} + \int_{t_2}^{t_f} \underline{\lambda}_{\Psi\Omega}^T \frac{\partial \underline{\underline{f}}}{\partial u} W^{-1} \left(\frac{\partial \underline{\underline{f}}}{\partial u}\right)^T \underline{\lambda}_{\Phi\Omega} dt \qquad \text{(A.3.9)}$$

$$I_{\Phi\Phi} = \int_{t_o}^{t_1} + \int_{t_2}^{t_f} \underline{\lambda}_{\Phi\Omega}^T \frac{\partial \underline{\underline{f}}}{\partial u} W^{-1} \left(\frac{\partial \underline{\underline{f}}}{\partial u}\right)^T \underline{\lambda}_{\Phi\Omega} dt \qquad \text{(A.3.10)}$$

The weighting factor $W^{-1}$ can be used to control integration between $t_1$ and $t_2$, that is, set $W^{-1} = 0$ when on the constraint boundary. All other variables used here are consistently defined in previous sections.

At the ends of the constraint boundary special procedures are necessary to handle changes in $t_1$ and $t_2$. Several alternate techniques to handle this difficulty are possible. The technique used in this report seems to work quite satisfactorily and is described in Appendix B.

# APPENDIX B

## COMPUTATION PROCEDURES

In the previous Appendix the analytical structure needed to solve for the optimal flight profile by the steepest descent method in the calculus of variations was developed. In this section, the numerical computing procedure used in the implementation of this method is presented. Since the experience gained in the development of the numerical program is generally applicable to the solution of other similar nonlinear optimal control problems, all significant operational problems and techniques are discussed.

### B.1 Basic Computing Procedure

The basic computing procedure used in the solution of the optimal flight profile is presented in this section, while the sections that follow go into more depth as to how the procedure was implemented. The procedure is as follows:

(a) Select and store an initial nominal control program which will result in a feasible and reasonable initial flight profile.

(b) Compute the nominal profile by integrating the state differential equations forward from the initial conditions to the stopping conditions, $\Omega = 0$, and store the state variables.

(c) Determine the values of the adjoint variables, $\underline{\lambda}$, by simultaneously evaluating $\underline{F}$ and integrating $\underline{\lambda}$ backwards from $\underline{\lambda}(s_f)$. At the same time calculate $\underline{G}$ and store $\underline{\lambda}_{\Phi\Omega}^T\underline{G}$ and $\underline{\lambda}_{\underline{\Psi}\Omega}^T\underline{G}$. Also, perform the integrations necessary to obtain the numbers $\underline{I}_{\underline{\Psi\Psi}}$, $\underline{I}_{\underline{\Psi}\Phi}$, and $I_{\Phi\Phi}$.

(d) Determine the gradient $d\Phi/dP$ and the error in the terminal conditions, $\underline{\Psi}$. If both are equal to zero, or nearly so, then the profile is at an optimum and computation is terminated; otherwise, continue.

(e) Calculate a value of $d\underline{\beta}$ which will improve the terminal conditions.

(f) Select a reasonable value of dP.

(g) Using the value of the variables above, determine the change in the control program, $\delta\underline{u}$, necessary to make a reduction in the performance index or to improve the terminal conditions.

(h) Obtain a new nominal control program, $\underline{u}_{new}$, by

$$\underline{u}_{new} = \underline{u}_{old} + \delta\underline{u}$$

Then continue the optimization procedure by restarting at (b).

## B.2 Computer Program

The procedure presented in the previous section was computerized using the MAD programming language and processed on the IBM 7094 computer at M.I.T. An outline of the computer program is shown in block diagram form in Figure 9. Each of the program blocks are discussed in the sections that follow. This block diagram schematically illustrates the procedure listed in Section B. However, since the Initialize Program routine, block 1, simply reads in constants, coefficients, and initial and final conditions required for the operation of the program, it will not be discussed. Block 4 is equally straight forward and will not be discussed either. The $\underline{D}$ and $\underline{E}$ matrices in block 5 are simplifying notations as follows:

$$\underline{D} = \underline{\lambda}_{\Phi\Omega}^{T}\underline{G}$$

$$\underline{E} = \underline{\lambda}_{\underline{\Psi}\Omega}^{T}\underline{G}$$

## B.3 Initial Nominal Control Program

This section presents a discussion of the selection of the initial nominal control program, $\underline{u}$, shown in program block 2 of Figure 9.

The choice of the initial nominal control program is theoretically unimportant if the function space of the problem is convex since the optimum profile can be reached from any

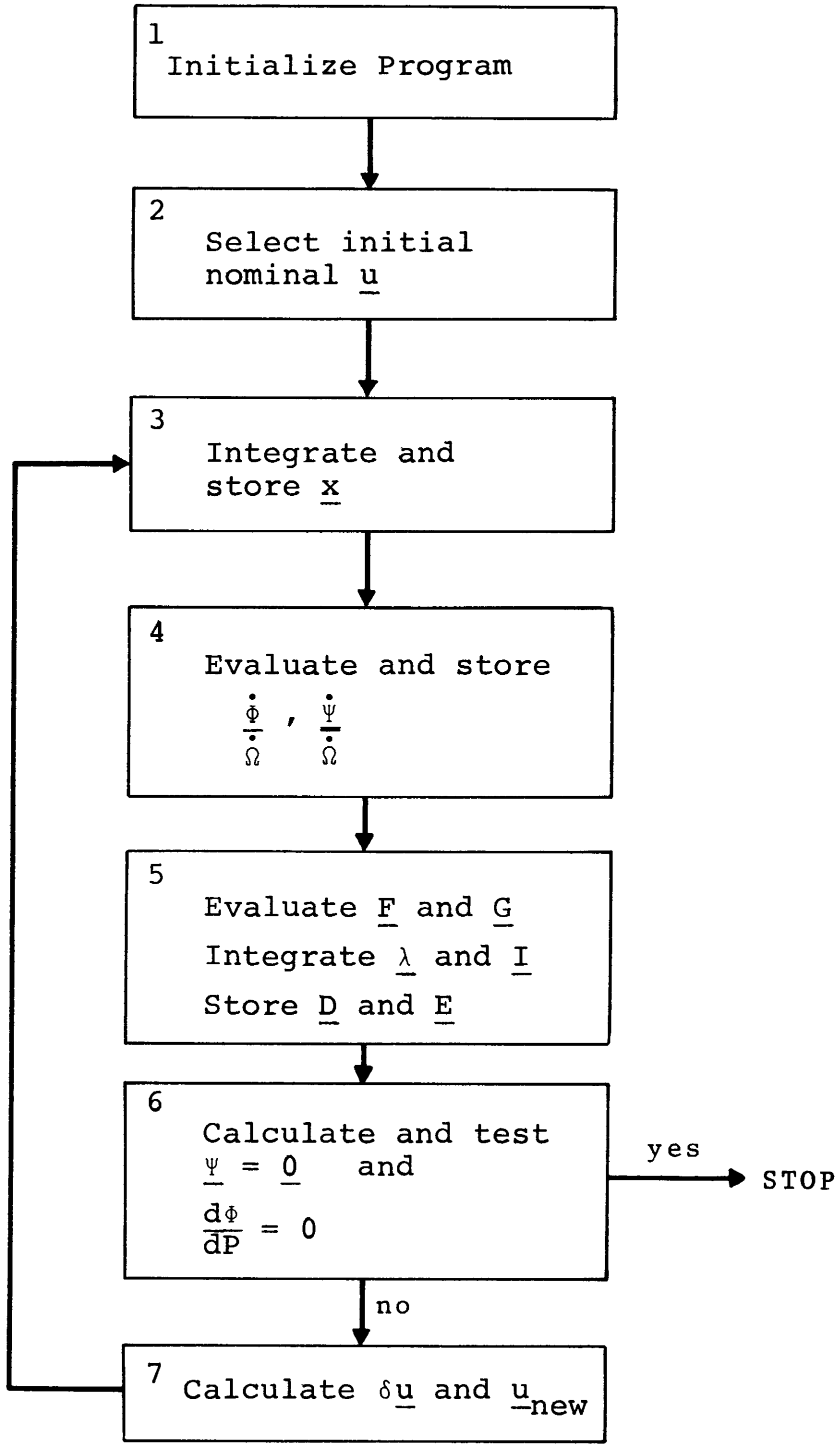


Figure 9. Computer Program Flow Diagram

location in that space. However, the efficiency of numerical solution of a nonlinear problem depends, to a great extent, upon the selection made. In an attempt to find a good nominal control, three initial control program techniques were tried.

The first was a technique of initially determining the optimal control program of a very short range flight. This required significantly less computing time to solve than the fifty mile range case. The proposed procedure was to use the proportionally streched optimal control program of the short range as a near optimal initial nominal for a slightly longer range. This procedure would be continued until the 50 mile optimum was achieved. Each of the short ranges selected were binary sub-multiples of 50 miles and range increases were accomplished by doubling the previous range. However, this technique proved to be less than desirable for this problem since each of the initial nominal control programs for an increased range were not near the optimum and, therefore, a significantly large amount of computing time was needed for each range case before the optimal for that range could be reached. It was concluded that starting with a good choice of an initial nominal at 50 miles would be more efficient.

With that in mind, an attempt was made at guessing a nominal control history which would result in a low value of the performance index while flying a reasonable flight profile. The guess was guided by an analytical technique which, unfortunately, could not take into account the dynamics of the system. Consequently, the flight profile was far from realistic since the altitude and velocity oscillated severely, the altitude went significantly negative at times, and all state variables satisfied the desired terminal conditions poorly. The later consequence was quickly and automatically rectified by the program, but the former situations resulted in a very nonlinear function space. The performance index obtained by this technique was very low and, in fact, near the optimal. However, the program progressed so slowly toward the optimum from this point in function space that, for all practical purposes, it did not move at all.

Both of the techniques discussed above for determining the initial nominal control program were abandoned in preference for the following technique which was much simpler to initiate and results in a function space which is more linear. This is desirable since the more linear the function space is, the faster the program moves toward the optimal. The technique was simply to fly the aircraft at the values of the initial conditions of the state variables over the 50 mile range. This resulted in a large value of performance index, but progress toward the optimal profile was effectively faster than the other two techniques.

## B.4 Integration Technique

Integration of the state variables, $\underline{x}$, the adjoint variables, $\underline{\lambda}$, and $\underline{I}$ shown as program blocks 3 and 5 of Figure 9 was carried out by the use of the Runge-Kutta fourth order integration technique using an integration interval, $\Delta s$. The general equations employed in the forward integration of the state variables are illustrated as follows:

$$\underline{x}_1' = \underline{f}(\underline{u}(s),\ \underline{x}(s))$$

$$\underline{x}_2' = \underline{f}\left(\frac{\underline{u}(s) + \underline{u}(s+\Delta s)}{2},\ \underline{x}(s) + \underline{x}_1' \frac{\Delta s}{2}\right)$$

$$\underline{x}_3' = \underline{f}\left(\frac{\underline{u}(s) + \underline{u}(s+\Delta s)}{2},\ \underline{x}(s) + \underline{x}_2' \frac{\Delta s}{2}\right)$$

$$\underline{x}_4' = \underline{f}\ (\underline{u}(s+\Delta s),\ \underline{x}(s) + \underline{x}_3'\ \Delta s)$$

$$\underline{x}(s+\Delta s) = \underline{x}(s) + \frac{\Delta s}{6}\ [\underline{x}_1' + 2(\underline{x}_2' + \underline{x}_3') + \underline{x}_4']$$

These integrations are performed from $\underline{x}(s_o)$ to the stopping condition, $\Omega = 0$.

The general equations employed in the backwards integration of the adjoint variables are also illustrated as follows:

$$\underline{\lambda}_1' = \underline{g}(\underline{u}(s),\ \underline{x}(s),\ \underline{\lambda}(s))$$

$$\underline{\lambda}_2' = \underline{g}\left(\frac{\underline{u}(s)+\underline{u}(s-\Delta s)}{2},\ \frac{\underline{x}(s)+\underline{x}(s-\Delta s)}{2},\ \underline{\lambda}(s)-\underline{\lambda}_1'\frac{\Delta s}{2}\right)$$

$$\underline{\lambda}_3' = \underline{g}\left(\frac{\underline{u}(s)+\underline{u}(s-\Delta s)}{2},\ \frac{\underline{x}(s)+\underline{x}(s-\Delta s)}{2},\ \underline{\lambda}(s)-\underline{\lambda}_2'\frac{\Delta s}{2}\right)$$

$$\underline{\lambda}_4' = \underline{g}(\underline{u}(s-\Delta s),\ \underline{x}(s-\Delta s),\ \underline{\lambda}(s) - \underline{\lambda}_3'\Delta s)$$

$$\underline{\lambda}(s-\Delta s) = \underline{\lambda}(s) - \frac{\Delta s}{6}[\underline{\lambda}_1' + 2(\underline{\lambda}_2' + \underline{\lambda}_3') + \underline{\lambda}_4']$$

These integrations are performed from $\underline{\lambda}(s_f)$ to $s_o$. The integration procedure used in obtaining $\underline{I}$ is essentially the same as for $\underline{\lambda}$.

To insure stability and accuracy of the numerical integrations, the size of the integration interval, $\Delta s$, was based on the criteria that the equivalent time step at all positions along the flight profile was to be less than one-tenth the period of the highest frequency component of the system, as well as less than the smallest time constant of any damped component of the system. The critical frequency component of this system was a 22 second phugoid oscillation of the aircraft at the initial and final flight conditions of 160 feet per second. Since the phugoid frequency decreases with speed, and since the aircraft is at 160 feet per second for only a very short time, a value of $\Delta s$ equal to 400 feet was selected even though this violated the previous criteria slightly.

## B.5 Test for Optimality

A test to determine if an optimal flight profile has been achieved is included in the optimization procedure as illustrated in block 6 of figure 9. Both the gradient and the terminal conditions are evaluated. If both are equal to zero, then the optimal profile has been achieved. However, for practical reasons, neither of these terms need be exactly zero. The question is, at what value of gradient and terminal conditions do you stop computing and accept the current profile as being optimal.

In the derivation of the gradient equation, A.2.29, the terminal conditions have been assumed to be satisfied exactly. However, it has been observed that the value of the gradient for the 50 mile flight profile case is relatively insensitive to small errors in the terminal conditions. Therefore, the terminal conditions were arbitrarily considered to be effectively zero if:

$$|\Psi_1| \leq 1 \text{ fps}$$

$$|\Psi_2| \leq .002 \text{ radians}$$

$$|\Psi_3| \leq 10 \text{ feet}$$

As for the gradient, an interesting relationship was observed for this problem. It was found that generally the gradient changed rather slowly when the program was making progress in reducing the performance index and, therefore, also making changes in $\underline{u}(s)$ and $\underline{x}(s)$. As the flight profile approached the optimum, this relationship was reversed; that is, little or no change in the values of $\Phi$, $\underline{u}(s)$ or $\underline{x}(s)$ were observed, but the value of the gradient decreased rapidly. After this condition was observed for several program passes, the program was stopped and the current flight profile was considered to be the optimum. It was found to be much more practical and effective to monitor the program visually, than to have the program automatically evaluate itself for optimal conditons.

## B.6 $\delta\underline{u}$ Calculation

If the flight profile is not optimal as evaluated above, then a change in the control program, $\delta\underline{u}$, is evaluated with the objective of reducing the performance index and/or improving the terminal conditions. A new nominal control program is then obtained by adding $\delta\underline{u}$ to the old program. As given by equation A.2.21, the determination of $\delta\underline{u}$ consists of terms which have been evaluated along the nominal profile (block 5 of figure 9), as well as three variables that we are at liberty to choose; $d\underline{\beta}$, dP and $\underline{W}^{-1}$. The manner in which these three variables are chosen is important to the stability of the numerical computation as well as the rate at which the optimization process proceeds towards the optimal.

The technique employed in the selection of these variables is the substance of discussion in this section.

Again referring to equation A.2.21, it is observed that the second term on the right-hand side is only used to make changes in the terminal conditions, and is accomplished by controlling the value of $d\underline{\beta}$. If no change is needed or desired, $\delta\underline{\beta}$ is set to $\underline{0}$. The function of the first term of this equation is to specify a change in $\underline{u}$ for the purpose of reducing the performance index. The magnitude of the control program change is specified by the value of dP, but tempered by the desired change in the terminal conditions, $d\underline{\beta}$, in the square root term. Care must be taken to insure that $d\underline{\beta}$ is not so large that the numerator of this term becomes negative. The value of dP was chosen to always insure that the system responded nearly linearly to $\delta\underline{u}$. Further discussion of this is presented later in this section.

The procedure used in making a change in the control program for this problem was to either make an effort to only decrease the performance index or to only improve the terminal conditions, but not both. This procedure made it easier to monitor the operation of the computer program and to detect the onset and cause of any computational instabilities. The program control policy was to always improve the terminal conditions in preference to reducing the performance index if any of the terminal conditions were poorly satisfied.

For most of the optimization process, the tolerated errors in the terminal conditions were set to fairly large values, since these errors made little difference in the ability to reduce the performance index. In fact, if only small errors had been tolerated, the computer program would have spent most of its time and effort correcting these errors since the terminal conditions always change by at least a small amount when effort is made to reduce the performance index. The maximum values of $|\underline{\Psi}|$ tolerated were 5 feet per second, .025 radians, and 100 feet for V, $\gamma$, and h respectively. Therefore, $d\underline{\beta}$ was set to $\underline{0}$ when all of the terminal errors were less than these values. When the flight profile was very near its optimal, then the tolerated values of the terminal errors were reduced to those specified in Section 6.5.

When only the terminal conditions were to be improved, the numerator of the square root term in equation A.2.21 was set to zero, and the value of $d\underline{\beta}$ was set equal to the terminal errors as follows:

$$d\underline{\beta} = - \underline{\Psi}$$

This procedure usually resulted in almost completely eliminating the terminal errors when the specified control purturbation, $\delta\underline{u}$, resulted in a linear response of the system. To insure linearity, the numerator of the square root term of equation A.2.21 was evaluated. Since the value of dP was always chosen to insure that the system responded nearly linearly to $\delta\underline{u}$, a negative value of the numerator indicated that the system would probably respond nonlinearly to the value of $d\underline{\beta}$ commanded. If this was the case, $d\underline{\beta}$ was repeatedly decreased by fifty per cent until the numerator was equal to or greater than zero. Several computer passes would then be required to satisfy the terminal conditions.

Whenever it was desired to change the performance index, $d\underline{\beta}$ was set to $\underline{0}$. Therefore, dP determined the magnitude of the perturbation in the control program, $\delta\underline{u}$. dP was evaluated on the basis of an approximate application of equation A.2.20 as follows:

$$dP = dP_K[(\Delta\underline{u}^T \; \underline{W} \; \Delta\underline{u})(s_f - s_o)]^{\frac{1}{2}}$$

where $\Delta\underline{u}$ was the nominal control change desired over the flight profile and was selected as

$$\Delta\underline{u} = \begin{bmatrix} \Delta C_L \\ \\ \Delta \text{Power} \end{bmatrix} = \begin{bmatrix} .1 \\ \\ 1000 \end{bmatrix}$$

The additional term, $dP_K$, is described further on in this section. The weighting factor, $\underline{W}$, compensates for the difference in magnitude of the two control variables and was selected as

$$\underline{W} = \begin{bmatrix} 1 & 0 \\ 0 & 10^{-8} \end{bmatrix}$$

The inverse of this term was used in equations A.2.21, .25, .26 and .27 and was held constant over the complete flight profile. Substituting the above values results in

$$dP = dP_K[\ .02\ s_f]^{\frac{1}{2}} = 72.6\ dP_K$$

since $s_f$ equals 50 miles and $s_o$ equals zero. This equation was an integral part of the computer program.

The addition of the $dP_K$ term in the equations above provided an easy method for changing the magnitude of $\Delta\underline{u}$ whenever desired. At the beginning of the optimization process it was arbitrarily set to 1.

Since it was important that the optimization process proceed toward the optimal flight profile rapidly, it was desirable to have dP set to as large a value as possible, but not so large that the system responded nonlinearly to the control program perturbation, $\delta \underline{u}$. The criteria used for determining linearity was to compare the actual change in the performance index with the change predicted by equation A.2.28. If the ratio of actual to predicted was greater than 1.50 or less than .67, then the system response to $\delta \underline{u}$ was considered to be too nonlinear and $dP_K$ was decreased by 50 per cent. If the ratio of actual to predicted was between .83 and 1.20, then the system perturbation was considered to be more linear than necessary and $dP_K$ was increased by 50 per cent. The criteria given above was established only after considerable experience with the program had been attained. It worked quite satisfactorily.

The last important topic in this section is the control of the weighting factor, $\underline{W}^{-1}$, in equations 2.2.21, .25, .26, and .27. As stated earlier, the inverse of weighting factor selected for the initial evaluation of dP was used in these four equations. The weighting factor specifies how the total control change will be distributed between the two elements of $\delta \underline{u}$ and, therefore, specifies the direction the system will move in function space. The initial value of $\underline{W}^{-1}$ stated earlier worked quite adequately at the beginning of the optimization process. However, as the process evolved, it was found that this distribution began to favor changes in $C_L$. The resultant consequence was that the rate of reduction of the performance index became very slow. In fact, the changes in $C_L$ became so large that the computational process became unstable. The most efficient and direct remedy to this problem was to visually monitor the magnitude of the calculated control changes, make value judgments as to if and how the distribution should be changed, and then to input a new weighting factor to the program when required. An important conclusion gained from the experience of controlling $\underline{W}^{-1}$ was that there is probably an optimum weighting factor, which may vary over the flight profile, that will maximize the rate of reduction of the performance index, $\Phi$. However, no theoretical technique was found that would determine this weighting factor.

## B.7 Inequality Constraints

If the flight profile optimization problem had no inequality constraints on the control variables, the description of the computing procedure would now be complete. However, since this is not the case, this section presents a brief description of the inequality constraint techniques used in this problem.

The computational theory applied when the control variables encountered boundary constraints is presented in section A.3. As implied by the integration intervals $t_1$ and $t_2$ in that section, the control variables are assumed to go on and come off the boundary constraints only once. To eliminate this restriction and to provide computational flexibility, a vector of flags associated with each control vector was established. A corresponding flag was then set at each integration step whenever a control variable was on the boundary. This resulted in a very simple program control and allowed the control variables to go on and come off of the constraint boundaries an unlimited number of times.

With this technique, the integrations of $\underline{I}$, equations A.3.8, .9, and .10, were handled very easily by simply setting the appropriate element of $\underline{W}^{-1}$ to zero whenever a control variable flag was found set, and then resetting that element of $\underline{W}^{-1}$ back to its previous value when off the boundary. The evaluation of $\delta\underline{u}$, equation A.3.7, was handled in the same manner. As derived in Section 2.3 the value of $\underline{\Delta F}$, equation A.3.4, was always zero. Therefore, no special computational procedure was required for the integration of $\underline{\lambda}$ when on any constraint boundary.

After the calculation of $\underline{u}_{new}$ it was necessary to determine if any segment of either control vector along the flight profile had encountered a constraint boundary. Therefore, each point of the control program along the flight profile was evaluated to determine if it had violated the inequality constraint, $\underline{C}$, equation A.3.1. If so, the appropriate control variable was set equal to the value of that boundary and the associated flag turned on. Special consideration must be given to allow the control variable to come off the constraint boundary. Several computerized techniques were tried but, unfortunately, each had draw-backs that resulted in computational unstability and in-efficiency. The procedure that was finally accepted was to monitor the program visually. By observing the shape of the control program, one could easily tell when and where the control program should come off the boundary. Releasing a control variable from a boundary was accomplished by simply setting the control flags in this region back to zero. As a measure of caution, the first and last few flags on a bounded control variable were occasionally set to zero even though it looked as though the variables would not have come off the boundary.